BIOCHEMISTRY

The linker domain of the initiator DnaA contributes to its ATP binding and membrane association in *E. coli* chromosomal replication

Yanqi Hou[1]†, Pankaj Kumar[2], Monika Aggarwal[3], Farzad Sarkari[1], Karen M. Wolcott[4], Dhruba K. Chattoraj[5], Elliott Crooke[1,3], Rahul Saxena[1]†*

Copyright © 2022 The Authors, some rights reserved; exclusive licensee American Association for the Advancement of Science. No claim to original U.S. Government Works. Distributed under a Creative Commons Attribution NonCommercial License 4.0 (CC BY-NC).

DnaA, the initiator of *Escherichia coli* chromosomal replication, has in its adenosine triphosphatase (ATPase) domain residues required for adenosine 5′-triphosphate (ATP) binding and membrane attachment. Here, we show that D118Q substitution in the DnaA linker domain, a domain known to be without major regulatory functions, influences ATP binding of DnaA and replication initiation in vivo. Although initiation defective by itself, overexpression of DnaA(D118Q) caused overinitiation of replication in *dnaA46*ts cells and prevented cell growth. The growth defect was rescued by overexpressing the initiation inhibitor, SeqA, indicating that the growth inhibition resulted from overinitiation. Small deletions within the linker showed another unexpected phenotype: cellular growth without requiring normal levels of anionic membrane lipids, a property found in DnaA mutated in its ATPase domain. The deleted proteins were defective in association with anionic membrane vesicles. These results show that changes in the linker domain can alter DnaA functions similarly to the previously shown changes in the ATPase domain.

INTRODUCTION

The family of AAA+ proteins [adenosine triphosphatases (ATPases) associated with diverse cellular activities] includes initiators of DNA replication, such as the bacterial DnaA protein and certain subunits of the eukaryotic origin recognition complex (ORC) (*1*). The *Escherichia coli* chromosomal replication initiator DnaA contains four domains (I to IV) (*2*, *3*), three of which have distinct but mutually dependent functions: domain I (residues 1 to 86) and domain III (residues 135 to 374) promote DnaA oligomerization (*3*–*5*) and recruit DnaB helicase (*6*). Domain I also interacts with other replication factors (*7*). Domain III, the AAA+ domain, binds adenosine 5′-triphosphate (ATP) and adenosine 5′-diphosphate (ADP) (*8*–*10*), hydrolyzes ATP (*11*), and interacts with acidic membranes (*12*, *13*). Domain IV (residues 375 to 467) binds specific DNA sequences (*14*). In addition to these structured domains, DnaA contains a flexible linker domain (domain II, residues 87 to 134) (*2*, *3*). The linker is believed to align domains I and III (*2*, *3*) and help in the optimal recruitment of DnaB helicase (*15*). No other roles of domain II are known.

Initiation of *E. coli* chromosomal replication occurs when multiple DnaA molecules oligomerize on a 245–base pair origin of replication (*oriC*) (*16*). The origin DNA wraps around the DnaA oligomer, which in the presence of the architectural protein Histone-like proteins (HU) and near physiological concentrations of ATP allows opening of an AT-rich region within *oriC* [termed DNA unwinding element (DUE)] (*5*, *17*, *18*). Once DUE is unwound, DnaB helicase and subsequently the rest of the replisome components are loaded onto the origin and replication commences (*3*, *6*).

Bacteria such as *E. coli* that are capable of rapid growth can do so by maintaining multiple copies of *oriC* and initiating from them simultaneously in a narrow window time (termed initiation synchrony) (*19*). Several *E. coli dnaA*ts mutants (e.g., those carrying the alleles *dnaA5* and *dnaA46*) although viable at permissive temperatures (≤30°C) show some degree of asynchrony in initiation (*20*). The well-studied *dnaA46*ts allele has two mutations that translate into Ala^{184} to Val (A184V) and His^{252} to Tyr (H252Y) substitutions in the DnaA protein (*21*, *22*). Another allele, *dnaA*cos, isolated as an intragenic suppressor of the *dnaA46*ts allele, allows cell growth up to 42°C but not at ≤30°C, referred to as cold-sensitive growth (cs) phenotype (*23*). The cs phenotype of *dnaA*cos cells results from hyperinitiation that causes aberrant replication elongation (*24*, *25*). The overexpression of SeqA protein, an inhibitor of replication initiation, suppresses the cs phenotype indicating a link between hyperinitiation and growth-arrested phenotypes (*26*).

In addition to mutations present in the *dnaA46*ts allele, the *dnaA*cos allele harbors two additional mutations that changes Gln^{156} to Leu and Tyr^{271} to His in DnaA (*25*, *27*). The A184V change common between the DnaA46ts and DnaAcos proteins causes defective ATP binding and lethality at elevated temperatures (the ts phenotype) (*22*, *27*). The temperature-resistance growth of *dnaA*cos cells is attributed to the Y271H change that appears to stabilize the activity of DnaAcos at elevated temperatures (*27*). In both *E. coli* wild-type (WT) (*27*) and *E. coli dnaA*(ts) (*4*, *28*) cells, increasing expression of *dnaA* WT gene from plasmids causes initiation asynchrony but does not prevent growth at the permissive temperature. In contrast, elevating expression of *dnaA46*ts or *dnaA*(A184V) mutant genes cause overinitiation and growth arrest at permissive temperatures (*28*).

The control of bacterial DNA replication initiation occurs primarily by regulating the activity of DnaA. DnaA has an intrinsic DNA-dependent ATPase activity. A mechanism termed regulatory inactivation of DnaA in which membrane-associated homolog of DnaA protein converts the active ATP-DnaA into inactive ADP-DnaA (*29*). In addition, specific DnaA-binding sites present at the chromosomal locus *datA* also accelerate ATP hydrolysis (*30*). The resulting drop

[1]Department of Biochemistry and Molecular and Cellular Biology, Georgetown University Medical Center, Washington, DC 20007, USA. [2]Center for Tuberculosis Research, Department of Medicine, Johns Hopkins University, Baltimore, MD 21287, USA. [3]Lombardi Comprehensive Cancer Center, Georgetown University Medical Center, Washington, DC 20007, USA. [4]Laboratory of Genome Integrity, Flow Cytometry Core Facility, Center for Cancer Research, National Cancer Institute, National Institutes of Health, Bethesda, MD, USA. [5]Basic Research Laboratory, Center for Cancer Research, National Cancer Institute, National Institutes of Health, Bethesda, MD, USA.
*Corresponding author. Email: rs426@georgetown.edu
†These authors contributed equally to this work.

in the cellular concentration of ATP-DnaA coupled with titration of ATP-DnaA by the newly synthesized DnaA-binding sites generated during replication elongation lowers free concentration of ATP-DnaA below the needed threshold (*3*). For chromosomal replication to initiate in daughter cells, cellular levels of ATP-DnaA must rise to the threshold level. It is believed to occur through the regeneration of ATP-DnaA from inactive ADP-DnaA in addition to de novo DnaA synthesis (*3*). In vitro, anionic phospholipids, particularly phosphatidylglycerol (PG) and cardiolipin (CL) present in the *E. coli* inner membrane, promote the release of adenine nucleotide bound to DnaA, which can then rebind ATP (*31*, *32*). There are specific intergenic sequences in the chromosome, known as DnaA reactivating sequences (DARS), which also promote rejuvenation of ADP-DnaA to ATP-DnaA, independent of CL (*33*).

An important and long-standing question that remains unanswered is why initiation in vitro requires ATP in concentrations similar to the physiological concentration, which is several orders of magnitude higher than that needed to saturate ATP binding to DnaA. ADP-DnaA but not ATP-DnaA generates relatively stable proteolytic fragments of various sizes when digested in the presence of near physiological concentrations of ATP (≥0.5 mM) (*34*), indicating a conformational shift between the two forms at high ATP concentrations. Mapping of the proteolytic fragments onto the amino acid sequences of DnaA identified several protease cleavage sites residing mainly in the ordered domains I and III as well as the linker domain (*34*). The high ATP concentration appears to promote conformational change in DnaA that is needed to make *oriC*-DnaA complex competent for replication initiation (*5*).

Live-cell imaging (*38*, *39*) and cell fractionation (*14*, *35*) studies indicate that DnaA is a membrane-associated protein. There is also evidence that membranes have a profound influence on DnaA activity (*3*). *E. coli* cell growth and normal chromosomal replication require proper levels of acidic phospholipids (PG and CL), as reduction in their levels results in inhibition of chromosomal replication and growth arrest (*36*, *37*). Cross-linking studies using a photoactivatable phospholipid analog revealed that a specific region of DnaA domain III inserts into the hydrophobic interior of the membrane bilayer (*13*). Acidic phospholipids in a fluid membrane protect the same region of DnaA, an amphipathic helix spanning residues 357 to 374, further supporting that this is the membrane-binding region of DnaA (*12*). Moreover, the growth-arrested phenotype of *pgsA* (the gene for PG synthase A, the enzyme for synthesis of acidic phospholipids) null cells can be suppressed by the overexpression of DnaA protein having certain small deletions and substitution in the membrane-binding domain, (*40*). One such substitution, DnaA(L366K), behaves like WT DnaA with respect to nucleotide binding, ATP hydrolysis, and specificity for PG and CL in promoting nucleotide exchange (*41*). While expression of DnaA(L366K) can restore growth of acidic phospholipid–deficient cells, it cannot serve as the only source of DnaA to initiate DNA replication in vivo (*40*) and in vitro (*42*); initiation requires some levels of WT DnaA. We found that DnaA(L366K), irrespective of its adenine nucleotide–bound state (*42*), produces replication-inactive DnaA-*oriC* structures, identical to what ADP-WT DnaA and not ATP-WT DnaA produces.

Previous studies using mutant DnaA proteins established that nucleotide and membrane binding are both functions of the AAA+ domain (*3*, *8*–*10*, *12*, *13*). Because of the lack of structural information of any full-length DnaA, alone or in complex with *oriC* DNA, it is not clear whether any other DnaA domains also contribute to nucleotide and membrane binding functions. Here, we constructed a three-dimensional model of full-length (domains I to IV) *E. coli* DnaA, using available partial structures of different DnaA homologs as templates (*9*, *10*, *43*). Docking of ATP onto the modeled structure indicated that a region of domain II, particularly the loop carrying Asp^{118} residue, lies near the nucleotide-binding pocket of domain III. Here, we show that the replacement of Asp^{118} with Gln drastically reduces the affinity of DnaA for ATP and the stoichiometry of binding. In vivo, DnaA(D118Q) mutant when overexpressed in the *dnaA46*ts host caused hyperinitiation and growth inhibition at the permissive temperature mimicking the phenotypes of DnaA(A184V), where the substitution is in the AAA+ domain. The growth arrest could be restored in both cases by overexpressing SeqA. DnaA deleted of specific residues in the linker domain mimicked the phenotype of DnaA(L366K) mutant, where the change is in the AAA+ membrane–binding region. These mutants bypass the PG requirement for cellular growth. The deletion mutants were also defective in association with anionic PG. These deletions when overexpressed, however, did not influence ATP binding and the viability of *dnaA46*ts host at the permissive temperature. The results reveal the functional importance of the linker domain because distinct changes there can alter functions that were seen due to changes in the AAA+ domain.

RESULTS

Modeling of DnaA structure suggests interaction between the linker and the ATP-binding domains of DnaA

We found that as opposed to ADP-DnaA, which is inactive as initiator, the active initiator ATP-DnaA is more susceptible to limited proteolysis when DnaA protein is mixed with the cellular levels of adenine nucleotides (*34*). Mass spectrometry analysis of proteolytic fragments identified a few ATP-DnaA–specific proteolytic sites, which resided in domain III and in domain II (the linker domain) of DnaA (*34*). ATP-induced allosteric change particularly in domain II is intriguing because domain III is the established ATP-binding AAA+ domain. These results suggest that there could be allosteric interdomain communication between domains II and III. Because no high-resolution structure of any full-length DnaA homolog is available, we constructed a full-length *E. coli* DnaA model (Fig. 1A) on the basis of the structure of *E. coli* DnaA domains I and II [Protein Data Bank (PDB) ID: 2E0G; (*43*)] and *Aquifex aeolicus* DnaA domains III and IV (PDB ID: 1L8Q) (*9*) using the Phyre2 server (*44*). The two truncated structures were merged using the Coot software (*45*) and energy-minimized using the Amber software (*46*). Modeling of ATP to the full-length structure was done on the basis of the structural constraints of AMPPCP (Adenylylmethylenediphosphonate disodium salt) binding in *A. aeolicus* DnaA [PDB ID: 2HCB; (*10*)].

Although the modeling studies were based on the available structures obtained at ATP concentrations lower than physiological concentrations, they served us well in revealing the structural rearrangements that may occur in the nucleotide-binding pocket upon nucleotide binding (*5*, *34*). Our modeled structure completely agrees with known crystal structures (*9*, *10*) when interactions between phosphate groups of ATP and conserved amino acid residues, such as Lys^{178} (Walker A) and Asp^{235} (Walker B), Ala^{184}, and Glu^{143} were correlated (Fig. 1B). In addition, we also recognized an earlier proposed interaction between the His^{136} residue with the hydroxyl

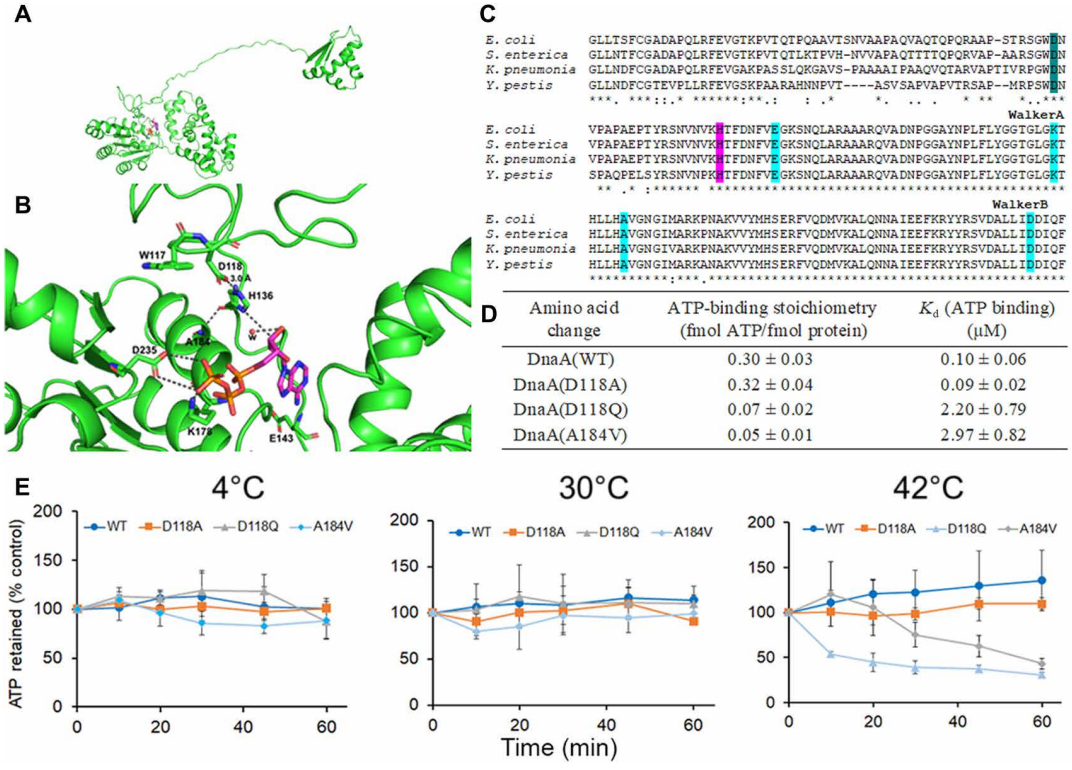

Amino acid change	ATP-binding stoichiometry (fmol ATP/fmol protein)	K_d (ATP binding) (μM)
DnaA(WT)	0.30 ± 0.03	0.10 ± 0.06
DnaA(D118A)	0.32 ± 0.04	0.09 ± 0.02
DnaA(D118Q)	0.07 ± 0.02	2.20 ± 0.79
DnaA(A184V)	0.05 ± 0.01	2.97 ± 0.82

Fig. 1. Asp^{118} residue of DnaA is important for ATP binding. (**A**) Homology-modeled structure of full-length *E. coli* DnaA protein. This was generated using the crystal structure of *E. coli dnaA* domain I (PDB ID: 2E0G) and *A. aeolicus* domains III and IV (PDB ID: 1L8Q) as templates. Docking of ATP was performed using crystal structure of *A. aeliocus* AMPPCP (PDB ID: 2HCB), and the final model was energy-minimized using the Amber software. (**B**) Enlarged view of domains II and III indicating positions of important amino acid residues forming the ATP-binding pocket. (**C**) Multiple-sequence alignment of DnaA protein homologs from Gram-negative γ-proteobacteria identifies Asp^{118} residue (colored in teal) as conserved. Other conserved amino acid residues (colored in turquoise) present within Walker A and B regions or outside those regions were known to be involved in ATP binding. His^{136} residue (colored in pink) that participates in DnaA oligomerization (*5*) is also indicated. (**D**) Stoichiometry and dissociation constant (K_d) of ATP binding of DnaA. WT and mutant DnaA proteins (0.15 to 0.9 μM) were incubated with 1 μM [α-32]-ATP, and nucleotide binding were measured by a filter retention assay. WT and mutant proteins (1.9 μM) were incubated with [α-32]-ATP (range between 0.005 and 2.5 μM) for 15 min at 4°C, and the nucleotide binding was measured by the filter retention assay to calculate K_d values. Mean (±SD) values from three independent experiments are shown. (**E**) To measure the stability of ATP binding of DnaA, WT and mutant DnaA proteins (1.9 μM) were mixed with ATP in PP-60 buffer (Materials and Methods) for 15 min at 4°C and incubated at 4°, 30°, or 42°C. Aliquots were collected at different time intervals (as indicated), and nucleotide binding was measured by the filter retention assay. Mean (±SD) values represent data from three independent experiments.

oxygen of ribose carbon at C2 position in ATP (Fig. 1B) (*5*). The present model also suggested that His^{136} might form hydrogen bonds with the backbone nitrogen of Ala^{184} (Fig. 1B). The model showed that the linker region, primarily a loop carrying the Asp^{118} residue, is in close proximity to His^{136}, and the two residues might be linked by hydrogen bond interactions. We previously reported that both Asp^{118} and His^{136} could be possible sites conferring ATP-dependent conformation changes (*34*). Multiple alignments using Clustal X 2.1 software (*47*) of primary amino acid sequences from different DnaA homologs belonging to γ-proteobacteria showed the evolutionarily conserved nature of these two amino acid residues (Fig. 1C).

DnaA with a specific substitution of Asp^{118} residue is defective in ATP binding

To investigate the importance of the Asp^{118} residue in DnaA function, we constructed DnaA mutants where the Asp^{118} residue was substituted with a nonconserved hydrophobic Ala and conserved hydrophilic Gln residues (table S3 and fig. S1, A and B). ATP-binding activity of the mutants was compared to that of DnaA WT (Fig. 1D). As a control, we used another mutant, DnaA(A184V), which is defective in ATP binding and where the changed residue is within the nucleotide-binding pocket of domain III (Fig. 1D). The results of filter retention assay indicate that the ATP-binding stoichiometries are similar for DnaA WT and DnaA(D118A) but significantly lower for DnaA(D118Q) (from ~0.30 ± 0.03 to 0.07 ± 0.02) (Fig. 1D). The control protein, DnaA(A184V), also showed similar reduction (from ~0.30 ± 0.03 to 0.05 ± 0.01) in ATP-binding stoichiometry (Fig. 1D) (*22*). Furthermore, ATP-binding affinity as indicated by dissociation constant (K_d) was comparable between DnaA WT and DnaA(D118A) but higher for DnaA(D118Q) (from ~0.10 ± 0.06 to 2.20 ± 0.79) and DnaA(A184V) (from ~0.10 ± 0.06 to 2.97 ± 0.82) (Fig. 1D and fig. S1B). We infer that the substitution of Asp^{118} with Ala does not affect ATP binding, but substitution with Gln significantly reduces the binding.

Unless challenged with acidic phospholipids such as CL, the ATP-DnaA complex remains intact (>90%) at 37°C for at least 60 min (*31*). When measured for up to 60 min, DnaA WT and DnaA(D118A)

proteins retained ATP at different temperatures comparably (4°, 30°, and 42°C) (Fig. 1E). DnaA(D118Q) also maintained its ATP form (with reduced affinity) at 4° and 30°C (Fig. 1E) but released the nucleotide at ≥37°C with a half-life ($t_{1/2}$) of ~10 min (Fig. 1E). Similar to DnaA(D118Q), DnaA(A184V) maintained its ATP form (with reduced affinity) at 4° and 30°C (Fig. 1E) and released the nucleotide at ≥42°C but with a slower kinetics than DnaA(D118Q) (Fig. 1E). These results suggest that the linker region containing Asp^{118} might be involved in retaining ATP in the nucleotide-binding pocket of domain III. We previously performed cross-linking experiments using DTSSP [3-3′-dithiobis(sulfosuccinimidylpropionate)] to confirm the ability of DnaA protein to produce the higher-oligomer forms required to make *oriC* competent for replication (*5*). We noted that when ATP-DnaA(D118Q) was treated with DTSSP, higher-order oligomer assemblies were not formed (fig. S2).

Substitution of Asp^{118} specifically with Gln reduces the thermostability of ATP-DnaA complex

The substitution of negatively charged Asp^{118} in the linker domain with conserved but uncharged Gln drastically reduces ATP binding of DnaA (Fig. 1D and fig. S1B). A possible explanation is that Gln at the 118th position adversely affects ATP-binding activity by disturbing the allosteric interdomain communication between the AAA+ domain and linker domain. Our in silico analysis predicts that the substitution of Asp^{118} by Gln might abrogate hydrogen bond formation with His^{136} of the AAA+ domain (compare fig. S3, A versus C). We performed additional homology modeling to examine how different substitutions of Asp^{118} residue might affect their interaction with His^{136}. This analysis predicted that another hydrophilic conserved residue, Asn if placed at position 118, may also interfere with the hydrogen bond formation with His^{136} (fig. S3D). Our in silico analysis also predicts that negatively charged Glu at position 118 moves away from His^{136} beyond the 3.5-Å distance that would inhibit formation of hydrogen bonds (fig. S4E).

We next performed ThermoFluor assays to assess how substitutions of Asp^{118} affect DnaA's stability. For this, Apo-DnaA and ATP-DnaA labeled with SYPRO Orange dye were gradually heated from 25° to 95°C (see Materials and Methods) to calculate their melting points (Fig. 2). The Apo-DnaA melted at 44°C (ground or inactive state), but the melting point for ATP-DnaA WT shifted to 57°C (Fig. 2) indicating an increase in stability upon ATP binding (stable or active state). There was no shift in melting points between DnaA(D118A) and DnaA WT, which suggests that the two DnaA proteins could be similar in structure and, hence, in their biochemical properties. The melting points for both DnaA(D118Q) and DnaA(A184V) were shifted to 49°C, indicating that both mutants are less stable than DnaA WT (Fig. 2). We have also generated a mutant DnaA protein where Asp^{118} is substituted with Gly, which relative to DnaA WT or DnaA(D118A) showed only a marginal decrease in the melting point (from 57° to 55°C). These results suggest that the replacement of Asp^{118} with a smaller amino acid residue may not affect DnaA stability, but a similar-sized and uncharged Gln substitution can partially destabilize DnaA protein and its ATP-binding activity. Moreover, substitution of Asp^{118} with Asn or negatively charged and bulkier Glu can completely destabilize the DnaA protein, as indicated by our inability to purify and characterize DnaA(D118N) and DnaA(D118E). In support of the in silico analyses, our results show the importance of Asp^{118} for the normal functioning of DnaA.

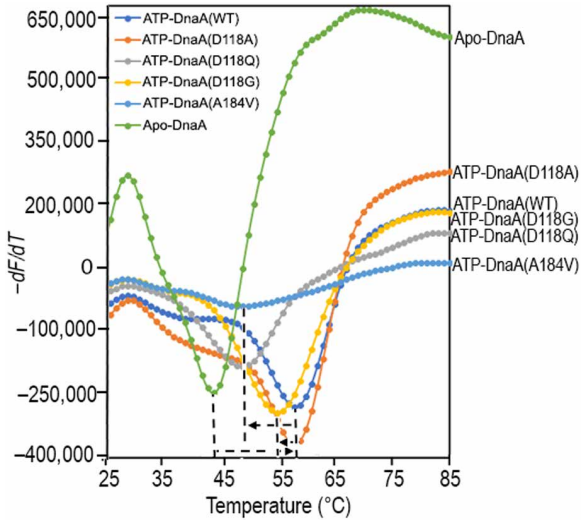

Fig. 2. Melting profiles of DnaA WT and its mutant derivatives. WT and mutant DnaA proteins (5 μM) mixed with ATP (5 mM) and incubated in ice for 15 min in a 96-well polymerase chain reaction plate. Three microliters of SYPRO Orange dye (at 50× dilution in water) was added in each well. The fluorescence data were collected between 25° and 95°C with temperature gradient set for 1 min/°. Melting temperature (T_m) and differential fluorescence (*–dF/dT*) values were calculated by fitting the data on sigmoidal dose-response (variable slope) equation in GraphPad Prism software. Experiments were performed in triplicate.

DnaA(D118Q) does not support *oriC*-dependent replication in vivo

The ATP-binding defect of DnaA(D118Q) prompted us to ask whether this mutant protein is also defective in the initiator function of DnaA. To test this, we used the Δ*dnaA* strain *E. coli* EH3827 (table S1), where initiation of chromosomal replication occurs from an integrated miniR1 plasmid (pKN500), which does not require DnaA for its own replication (*48*). EH3827 cells bearing the empty vector pBAD (*49*) or the same vector carrying the WT (*40*) or mutant *dnaA* genes *dnaA*D118A, *dnaA*D118Q, or *dnaA*A184V (as in plasmids pZL606, pRS18, pRS19, or pRS20, respectively), where the genes are under an arabinose-inducible promoter, were transformed with a p*oriC* plasmid (table S2). The transformation mixtures were plated on LB-agar plates supplemented with appropriate antibiotics in the absence or presence of arabinose. Cell viability was measured in the absence of arabinose or in the presence of 0.2% glucose (to prevent leaky expression) and without selection for the p*oriC* plasmid (Table 1). Similar number of transformants were seen upon inclusion of arabinose (0.2%) in the medium, indicating that expression of the various *dnaA* genes by itself had no adverse effect on cell viability when p*oriC* was not selected (Table 1). The overproduction of different DnaA proteins in the presence of 0.2% arabinose was confirmed by Western blotting (fig. S4).

Whereas bacterial cells carrying the empty vector did not show transformants at any arabinose concentration used, cells overexpressing DnaA WT showed an increasing number of transformants with increasing inducer concentrations (Table 1). Similar increase in the number of the transformants was also seen for cells overexpressing DnaA(D118A) (Table 1). In contrast, cells carrying DnaA(D118Q) or DnaA(A184V) showed at least 50-fold reduction in the number of transformants when 0.1 or 0.2% arabinose was included in the media (Table 1). In all cases, no transformants were found when

Table 1. DnaA(D118Q) makes chromosomal replication initiation defective in vivo. *E. coli* EH3827 (Kn^R resistance) cells were transformed with empty pBAD vector and its derivatives: pZL606 carrying *dnaA*(WT), pRS18 carrying *dnaA*(D118A), pRS19 carrying *dnaA*(D118Q), and pRS20 carrying *dnaA*(A184V) under an arabinose-inducible promoter and plated on LB-agar plates supplemented with ampicillin. Bacterial cells were made competent and further transformed with a plasmid containing *oriC*. The mixture was plated after appropriate dilution (~1000-fold) where p*oriC* is not selected, and 100 μl of transformation mixture on LB-agar plates supplemented with indicated amount of arabinose (0.05, 0.1, and 0.2%) and appropriate antibiotics (Ap + Cm or Kn + Cm), and plates were incubated for 16 to 36 hours. Cells plated on LB-agar plates containing no arabinose or 0.2% arabinose or 0.2% glucose but no antibiotic to select p*oriC* maintenance served as positive control. Cells plated at LB-agar plates containing no inducer (only Ap + Cm) or antibiotic selection to maintain pBAD plasmids (Kn + Cm) served as negative control. Data represent average values from at least three biological replicates. Ap, Ampicillin; Cm, Chloramphenicol; Kn, Kanamycin.

***E. coli* EH3827 with**	**Number of colonies/μg DNA**							
	Ap			**Ap + Cm**			**Ap + Cm**	**Kn + Cm**
	0 Ara/Glu	**0.2% Glu**	**0.2% Ara**	**0.05% Ara**	**0.1% Ara**	**0.2% Ara**	**0 Ara/Glu**	**0 Ara/Glu**
pBAD	$7.2 \pm 0.9 \times 10^6$	$6.9 \pm 0.9 \times 10^6$	$7.2 \pm 1.0 \times 10^6$	<1	<1	<1	<1	<1
pdnaA	$6.7 \pm 1.0 \times 10^6$	$6.8 \pm 0.8 \times 10^6$	$6.8 \pm 0.9 \times 10^6$	$<10^2$	$5.3 \pm 1.4 \times 10^3$	$5.0 \pm 1.0 \times 10^4$	<1	<1
*pdnaA*AD118A	$7.7 \pm 1.7 \times 10^6$	$7.6 \pm 1.5 \times 10^6$	$7.7 \pm 1.6 \times 10^6$	$<10^2$	$5.0 \pm 0.9 \times 10^3$	$4.7 \pm 0.3 \times 10^4$	<1	<1
*pdnaA*AD118Q	$7.3 \pm 1.7 \times 10^6$	$7.6 \pm 1.7 \times 10^6$	$7.3 \pm 1.6 \times 10^6$	<1	$\sim 10^2$	$1.0 \pm 0.5 \times 10^3$	<1	<1
*pdnaA*AD184V	$7.8 \pm 2.1 \times 10^6$	$7.9 \pm 2.1 \times 10^6$	$7.9 \pm 2.0 \times 10^6$	<1	$\sim 10^2$	$1.0 \pm 0.3 \times 10^3$	<1	<1

oriC was selected, but DnaA expression was not induced indicating the requirement of DnaA for maintenance of p*oriC*, as expected (Table 1). Together, these results indicate that DnaA(D118Q) is significantly defective in initiator function, similarly to DnaA(A184V).

Overexpression of DnaA(D118Q) in cells with chromosomal *dnaA46*ts allele causes inviability

We next considered the possibility that although D118Q is significantly defective in replication initiation, it might rescue defects of other initiation-defective mutants by forming functional mixed oligomers. For example, although bacterial cells carrying the *dnaA46*ts allele cannot grow at 42°C (*23*, *25*), overexpression of DnaA WT from a plasmid can rescue the growth defect at high temperature (*27*). Similar level of expression of DnaA(A184V) from a plasmid also rescues the growth defect at high temperature, but unlike the expression of DnaA WT, cells become cold sensitive (inviable) when DnaA(A184V) is overexpressed (*25*, *28*).

Considering the similarity in the ATP-binding defect of DnaA (D118Q) and DnaA(A184V), we wanted to test whether similar to the DnaA(A184V) mutant, DnaA(D118Q) could also rescue growth of *dnaA46*ts cells. We found that *E. coli dnaA46*ts cells bearing the empty vector pBAD or the same vector carrying *dnaA* WT or its mutant derivatives *dnaA*(D118A) (as in pRS18) did not show any growth defect at 30°C at all inducer concentrations (Table 2). Induced expression of DnaA(D118A) also allowed growth at 42°C as was known for DnaA WT (*27*).

In contrast to DnaA WT and DnaA(D118A), the behavior of DnaA(D118Q) was different. It supported growth of *dnaA46*ts at 30°C at low inducer concentration (0.05% arabinose) but not at higher inducer concentrations, 0.1 or 0.2% (Table 2). However, at 42°C, cells could tolerate the expression of DnaA(D118Q) when the inducer was 0.05 or 0.1% but not 0.2% (Table 2). These results are reminiscent of the phenotypes of DnaA(A184V) overexpression in *dnaA46*ts cells, i.e., conferring to the host thermal resistance at 42°C and inhibition of growth at 30°C. We also induced DnaA(D118Q) expression in the WT host (*E. coli* MG1655) instead of the *dnaA46*ts host, and there was no growth defect of the host at 30°C (table S4). This suggests that *dnaA*D118Q is recessive to DnaA WT but not to the *dnaA46*ts allele.

Overexpression of DnaA(D118Q) in *dnaA46*ts host causes hyperinitiation

The inviability of *dnaA46*ts cells at nonpermissive temperatures is apparently due to A184V substitution, because it causes an ATP-binding defect in DnaA (*22*). The earlier results showing the ATP-binding defect of DnaA(D118Q) (Fig. 1D) could be one reason for the failure of the mutant to compensate for the ATP-binding defect of DnaA(A184V) and to support growth of *E. coli dnaA46*ts at high temperature. The failure to support growth of *dnaA46*ts by DnaA(D118Q) at 30°C could, however, be from hyperinitiation, as was the case with the *dnaA*cos mutant at low temperature (*23*–*25*). To test this possibility, we measured chromosomal DNA content by flow cytometry. *E. coli dnaA46*ts cells (Str^R) were transformed with plasmid vector pBAD (Ap^R) or pBAD carrying one of the genes: *dnaA*, *dnaA*(D118A), *dnaA*(D118Q), or *dnaA*(A184V). The transformants were plated on LB-agar plate supplemented with ampicillin and streptomycin at 30°C. The single transformants from each plate were grown at 30°C to exponential phase [optical density at 600 nm (OD_{600}) of 0.15], and their DNA content was analyzed by flow cytometry after blocking replication initiation with rifampicin and allowing time to already initiated chromosomes to complete replication elongation. Without induction of DnaA, replication initiation was asynchronous but to a comparable degree in all cases (Fig. 3). Upon induction of DnaA (fig. S5), overreplication was apparent in all DnaA overexpressing cells, but it was more extensive in the case of DnaA(D118Q) and DnaA(A184V) mutants, the two that inhibit growth (colony formation) at the permissive temperature (Table 2). We note that in liquid media, cells grew initially (up to an OD_{600} of 0.1 to 0.15) even in the presence of the inducer (arabinose), most likely because it takes time for the mutant proteins to accumulate to a threshold level. These two mutants again showed higher DNA content per cell when exponentially growing cultures were treated without rifampicin and cephalexin (fig. S6A) or with only cephalexin (fig. S6B). Thus, although defective in replication initiation by itself, DnaA(D118Q) can cooperate with DnaA46(ts) to promote replication initiation even more than what DnaA WT can with DnaA46(ts). Together, these results confirm that *dnaA46*ts cells hyperinitiate when DnaA(D118Q) is overexpressed.

Table 2. DnaA(D118Q) inhibits growth of the *dnaAts* mutant. *E. coli* CM742 (*dnaA46ts*) cells transformed with plasmids bearing empty vector pBAD and its derivatives pZL606 carrying *dnaA*(WT), pRS18 carrying *dnaA*(D118A), pRS19 carrying *dnaA*(D118Q), and pRS20 carrying *dnaA*(A184V), and cells were plated on LB-agar plates containing ampicillin and streptomycin. Single transformants were grown to an OD_{600} of ~0.1, and after appropriate dilution (~1000-fold), cells (100 μl) were plated on LB-agar plates supplemented with arabinose (0.0, 0.05, 0.1, and 0.2%). Plates were incubated at 30°C or at 42°C for 16 to 24 hours. Cells plated on LB-agar plates containing no arabinose or 0.2% glucose served as control. To calculate transformation efficiency, colony numbers in the presence of no inducer at 30°C were taken as 1000, and the other values were normalized to 1000. Data represent average values from at least three biological replicates.

E. coli CM742 with	Relative number of colonies at									
	30°C					42°C				
	0 Ara/Glu	0.05% Ara	0.1% Ara	0.2% Ara	0.2% Glu	0 Ara/Glu	0.05% Ara	0.1% Ara	0.2% Ara	0.2% Glu
pBAD	1000	1023 ± 323	1050 ± 74	1098 ± 241	1003 ± 145	<1	<1	<1	<1	<1
pdnaA	1000	1124 ± 283	1100 ± 174	1083 ± 234	1070 ± 131	<1	1189 ± 218	1122 ± 162	1139 ± 130	<1
*pdnaA*D118A	1000	1016 ± 316	954 ± 151	1112 ± 106	1115 ± 107	<1	980 ± 229	996 ± 215	976 ± 317	<1
*pdnaA*D118Q	1000	980 ± 160	<1	<1	1081 ± 77	<1	1049 ± 157	993 ± 235	140 ± 85	<1
*pdnaA*D184V	1000	991 ± 43	<1	<1	1061 ± 143	<1	939 ± 138	942 ± 180	534 ± 150	<1

Overexpression of SeqA, a negative regulator of replication initiation, can overcome the growth defect of *dnaA*cos cells and such cells show reduced DNA content per cell (*28*). To test whether SeqA can rescue growth defect of *dnaA46*ts cells at permissive temperature due to overexpression of DnaA(D118Q), we developed a two-plasmid system where one carried *dnaA* or its mutant derivative genes under an arabinose-inducible promoter and the other carried the *seqA* gene under an isopropyl-β-D-thiogalactopyranoside (IPTG)–inducible promoter (see Materials and Methods). The SeqA expressing plasmid, pRD, was a derivative of plasmid pACYC184 (table S2) (*50*). Cells containing pRD and plasmid vector pBAD (Ap^R) or pBAD carrying one of the genes [*dnaA*, *dnaA*(D118A), *dnaA*(D118Q), or *dnaA*(A184V)] showed no apparent differences in expression of different DnaA proteins in the absence or presence of SeqA protein (fig. S7, A and B). However, cells carrying *dnaA*(D118Q) or *dnaA*(A184V) now showed growth at 30°C when plated on LB-agar plates containing IPTG (50 μM) both in the absence of arabinose or in the presence of 0.2% arabinose or 0.2% glucose (table S5). This indicates that as long as SeqA is expressed, overexpression of DnaA(D118Q) or DnaA(A184V) does not prevent growth. We also note that without addition of IPTG (i.e., no SeqA overexpression), colonies were seen on arabinose containing plates, i.e., under conditions of overexpression of DnaA(D118Q) and DnaA(A184V) (table S5). This is attributed to possibly leaky expression of SeqA in the absence of IPTG (table S5). In line with these results, flow cytometry measurements showed reduced DNA content in all DnaA-overexpressing cells in the presence of SeqA protein (Fig. 4). In summary, the results are consistent with our inference that overreplication as the underlying reason of lethality of *dnaA*ts cells upon overexpression of the D118Q mutant. The similarity in the behavior of DnaA(D118Q) and DnaA(A184V) mutants indicates that a change in the previously unappreciated linker domain can affect initiation as significantly as a change in the AAA+ domain.

Short deletions in the linker domain make anionic membranes dispensable for cell growth

Multiple-sequence alignment of DnaA homologs from members of γ-proteobacteria including *E. coli*, *Salmonella enterica*, and *Klebsiella pneumonia* revealed 100% identity in amino acid residues of the structured domains. The linker domain showed 56% identity (with overall 80% similarity), which is more pronounced in the proximal half of linker region (Fig. 5A). The sequence conservation suggests that the linker region could be serving some specific functions. The linker regions also have charged amino acid residues carrying low hydrophobicity and a lower degree of complexity as intrinsically disordered regions (IDRs) (*51*). Amino acids, such as A, R, D, Q, S, and P, which are hydrophilic or charged have the propensity to promote disordered structures, while amino acids W, F, Y, I, L, and C, which are hydrophobic and uncharged, can promote ordered structures (*52*). We noticed that the amino acid residues characteristic of IDRs are also present in the DnaA linker region (Fig. 5B). Using ANCHOR2 (*53*) and IUPred2 (*51*) tools, we predicted that IDRs in DnaA reside in two patches, between residues 66 to 131 and 351 to 375 (Fig. 5C). The latter region was previously shown to be involved in DnaA-membrane interactions (*12*, *13*). This led us to wonder whether other putative IDR in the linker domain could also have a role in DnaA-membrane association. Because the mutant forms of DnaA, such as DnaA(L366K), can overcome PG deficiency, this suggests that the mutations are conferring a gain of function to DnaA by mimicking allosteric modification that is normally induced upon interactions with PG. The membrane-association function has also been mutationally uncoupled from the ATP-binding function DnaA (*8*–*10*, *12*, *13*, *41*). We were also interested to know whether the putative IDR in the linker domain is also involved in membrane association and whether this function is independent of ATP-binding function of the linker domain.

To examine this, we constructed a series of mutants by systematically deleting five consecutive amino acids at a time in the region spanning residues 87 to 134 (table S3). WT and the mutant *dnaA* alleles were cloned under the control of an arabinose-inducible P_{BAD} promoter in plasmid pBAD24c. We used *E. coli* HDL1001 cells where the chromosomal *pgsA* gene, required for the synthesis of acidic phospholipids, is under the control of the IPTG-inducible *lac* promoter (*40*). Removal of IPTG from a fully induced culture causes growth arrest after approximately 8 to 10 generations with a concomitant 10-fold reduction in the cellular levels of the acidic phospholipids,

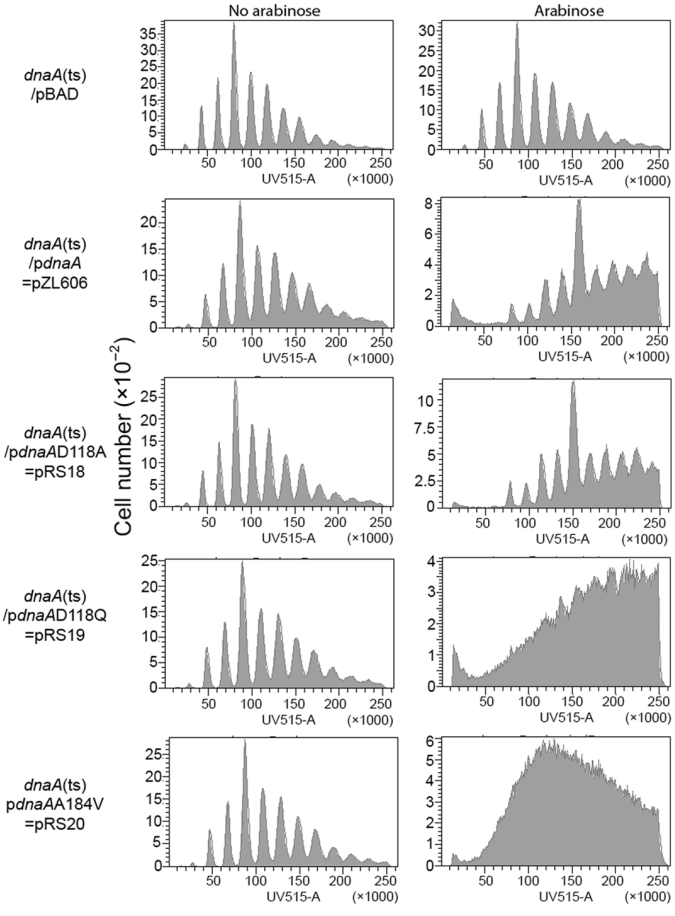

Fig. 3. The DnaA(D118Q) mutant causes hyperinitiation. Total DNA content per cell was measured by flow cytometry. *E. coli* CM742 cells were transformed with pBAD24c derivative plasmids expressing WT (pZL606) or mutant DnaA proteins: DnaA(D118A) (pRS18), DnaA(D118Q) (pRS19), and DnaA(A184V) (pRS20) from an arabinose-inducible promoter. Cells were grown in LB medium containing either 0.2% glucose or 0.2% arabinose at 30°C to an OD_{600} of ~0.15 and treated for 2.5 hours with rifampicin to stop replication initiation and cephalexin to stop cell division. Replication runout profiles indicate the number of chromosomal origins per cell at the time of drug treatment.

PG and CL (*40*). *E. coli* HDL1001 cells were transformed with pBAD24c vector alone or the vector bearing WT or mutant *dnaA* genes and plated on LB-agar plates, supplemented with appropriate antibiotics. Whereas plates without IPTG did not show any colony-forming units, the addition of 1 mM IPTG resulted in cell growth with no apparent differences in the colony-forming units among any of the *dnaA* variants (Fig. 5D). These results confirm that the growth of HDL1001 cells depends on IPTG-dependent *pgsA* expression. LB-agar plates supplemented with 0.2% arabinose but no IPTG showed colony-forming units with cells expressing DnaA proteins carrying short deletions in the linker region: DnaA(ΔS112-G116), DnaA(ΔA122-P126), and DnaA(ΔT127-131N). No colonies were present on LB-agar plates containing 0.2% glucose, which is expected from the tight repression of P_{BAD} promoter by glucose (Fig. 5D). Together, our results suggest that these short regions play functionally important roles in the DnaA-membrane association.

DnaA with short deletions in the linker domain retain ATP binding and their overexpression does not prevent growth of *dnaA46*ts cells at the permissive temperature

We purified DnaA WT and its short deletion derivatives (fig. S8A and tables S2 and S3) to examine how they bind ATP. DnaA WT and the mutants (at ~0.15 to 0.9 μM) were incubated with 1 μM [α-32]-ATP, and ATP binding was measured by the filter retention assay. While the ATP-binding stoichiometry for the WT was 0.31 ± 0.02, the stoichiometries for the mutants were 0.15 ± 0.03 for DnaA(ΔS112-G116), 0.16 ± 0.05 for DnaA(ΔA122-P126), 0.20 ± 0.04 for DnaA(ΔT127-N131), and 0.31 + 0.03 for DnaA(L366K) (Fig. 6A). The mutants thus appear to cause some ATP retention defect. To calculate K_d values, DnaA proteins (at 1.9 μM) were incubated with different concentrations of [α-32]-ATP (0.005 to 2.5 μM). The results indicate that the mutants retain high affinity for ATP binding similar to DnaA WT protein (Fig. 6A and fig. S8B). In contrast, the complete deletion of DnaA domain II (amino acid residues 87 to 134) drastically reduced the ATP-binding stoichiometry (0.03 ± 0.02) as well as affinity (K_d = 3.08 ± 0.72) (Fig. 6A and fig. S8B). Thus, a larger deletion in the linker domain can cause more significant defect in ATP binding.

Considering that the DnaA deletions are in the vicinity of Asp^{118}, we wanted to test whether like the DnaA(D118Q) mutant, overexpression of the deletion mutants could cause defective growth of *dnaA46*ts cells. For this, the deleted alleles were cloned in the pBAD vector, and the derivatives were used to transform *E. coli* CM742 (*dnaA46*ts) (tables S1 to S3). The transformants were plated on LB-agar carrying appropriate antibiotics in the absence or presence of 0.2% arabinose or in the presence of 0.2% glucose. We found that *dnaA46*ts cells bearing the empty vector pBAD or the same vector carrying *dnaA* or its mutant derivatives did not show any growth defect at 30°C both in the absence and presence of inducers (Fig. 6B). In line with this observation, *dnaA46*ts cells carrying the deletion mutants showed only small changes in DNA contents upon induction with arabinose (Fig. 6C and fig. S9). The behavior of the three mutants were essentially similar and very different from DnaAD118Q, which causes overreplication and growth arrest unlike the deletion mutants.

The short deletions in the linker domain alter DnaA-membrane association

As shown above, deletion of specific residues from the DnaA linker domain allows *E. coli* growth with reduced anionic phospholipids. This may suggest that the deleted regions play an inhibitory role in the absence of PG. To test this, we transformed the *E. coli* EH3827 (=Δ*dnaA*/*pgsA*$^+$) (table S1) with pZL606 (carries *dnaA* WT under P_{BAD}). Following separation from the cytosolic protein fraction (as described in Materials and Methods), the membrane fraction was solubilized using detergents 1-*S*-octyl-β-D-thioglucopyranoside [octyl-thio-glucoside (OTG)] or [3-((3-cholamidopropyl) dimethylammonio)-1-propanesulfonate]. The soluble and detergent-solubilized fractions were resolved by SDS–polyacrylamide gel electrophoresis (SDS-PAGE), transferred to a nitrocellulose membrane, and probed with polyclonal α-DnaA antiserum (fig. S10). As expected, no band related to DnaA protein was present in either the cytosolic or the membrane-solubilized fractions of the Δ*dnaA* strain, EH3287. On the other hand, EH3287 cells overexpressing DnaA WT showed DnaA both in the cytosolic and membrane fractions. Next, we transformed *E. coli* EH3287 cells with pZL607 (carrying *dnaA*L366K allele), pSR7

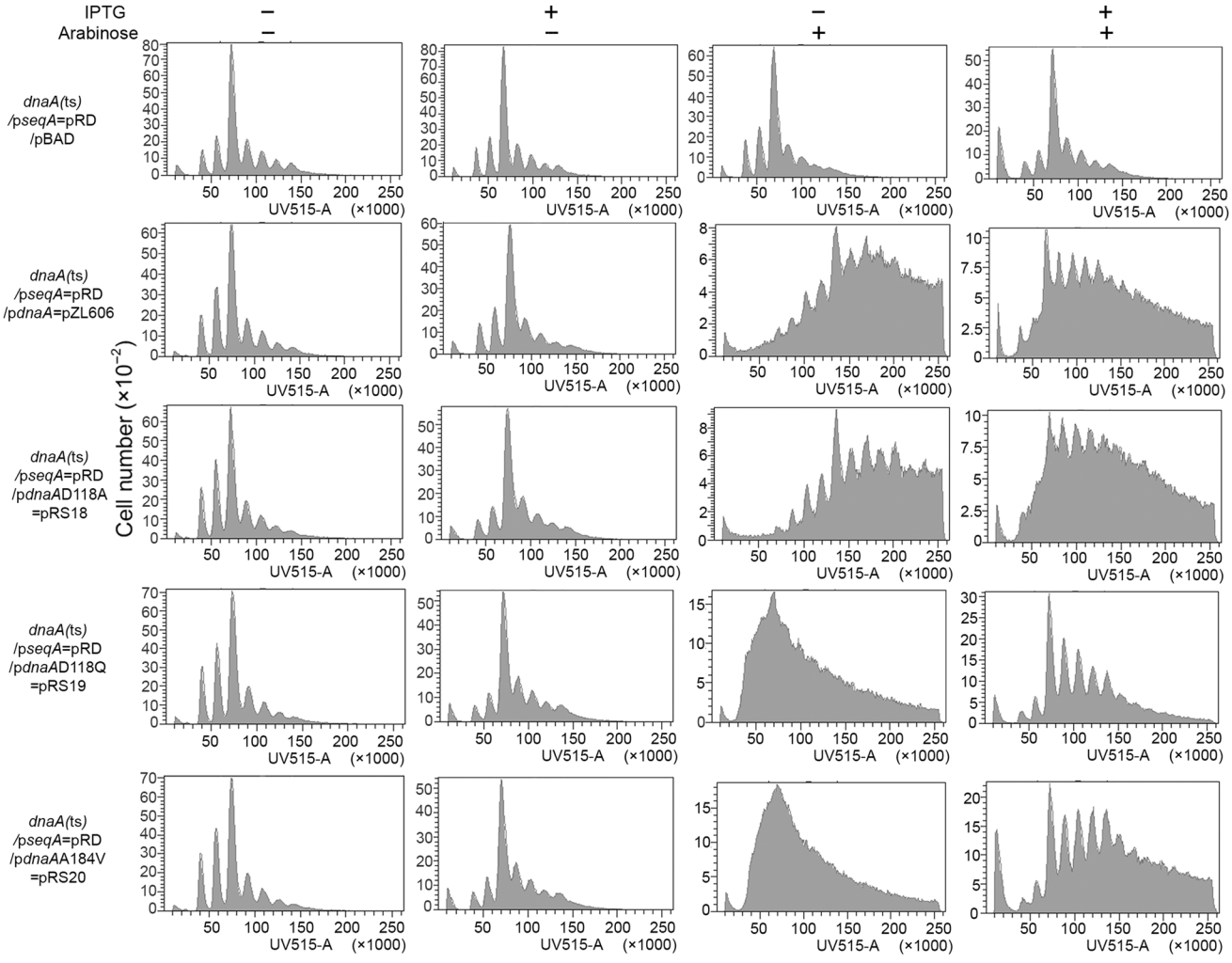

Fig. 4. Overexpression of SeqA prevents overinitiation by some of the mutant DnaA proteins. *E. coli* CM742 cells carrying plasmid pRD, where the *seqA* gene is under an IPTG-inducible promoter, were transformed with vector pBAD and its derivatives (pZL606, pRS18, and pRS19) expressing WT or mutant DnaA proteins from an arabinose-inducible promoter. Otherwise, the details are the same as in Fig. 3.

(carrying *dnaA*ΔS112-G116 allele), pSR9 (carrying *dnaA*ΔA122-P126 allele), or pSR10 (carrying *dnaA*ΔT127-131N). The membrane-bound (OTG-solubilized) and cytosolic fractions were analyzed for the DnaA content. Immunoblotting revealed that DnaA WT, DnaA(L366K), and DnaA(ΔA122-P126) were retained in the OTG-solubilized membrane fractions, while DnaA(ΔS112-G116) and DnaA(T127-131N) were not (Fig. 7A). Probing the cytosolic fractions demonstrated that the WT and mutant DnaA proteins were similarly overexpressed within a twofold range (Fig. 7B). Immunoblotting of OTG-solubilized membrane fractions of cells overexpressing DnaA(D118Q) showed abundant accumulation in the membrane, but similar levels of protein in the cytosol when compared with WT (fig. S11). These results are consistent with direct interactions of the linker region with membrane, and this can play significant regulatory role in interactions with PG: The regions deleted in the linker region possibly plays a positive role in WT cells, but the role of those regions appears to become inhibitory in the absence of PG.

Anionic phospholipids such as PG, but not zwitterionic phospholipids such as phosphatidylcholine (PC), when mixed with ATP-DnaA protein result in release of the bound nucleotide (*41*). We performed a ThermoFluor assay to examine the interaction of anionic phospholipids with WT or mutant DnaA proteins that suppress the requirement of anionic phospholipids for cellular growth. We selected Apo-DnaA protein (ground or inactive state with a melting point of 44°C) as a negative control and ATP-DnaA protein (a stable or active state with a melting point of 57°C) as a positive control. We found that ATP-bound forms of DnaA(WT), DnaA(ΔS112-G116), DnaA(ΔA122-P126), and DnaA(ΔT127-N131) have essentially the same melting point (approximately 57°C), while DnaA(L366K) exhibits a slightly lower melting point (from 57° to 54°C) (Fig. 7C). To examine the DnaA-lipid interaction, we prepared small unilamellar vesicles (SUVs) composed of DOPG [1,2-dioleoyl-*sn*-glycero-3-phospho-(1′-rac-glycerol)]. ATP-DnaA(WT) when mixed with 25 μM SUVs (Fig. 7D), exhibited two peaks (at 44° and 57°C): one corresponding to the melting point of Apo-DnaA (at 44°C) and the other to that of ATP-DnaA (at 57°C). When the SUV concentration was increased to 100 μM, the 57°C peak shifted to 44°C peak position (Fig. 7E). Inclusion of 25 μM SUV shifted ATP-DnaA(L366K) peak from 54° to 50°C (Fig. 7, C versus D), which did not shift

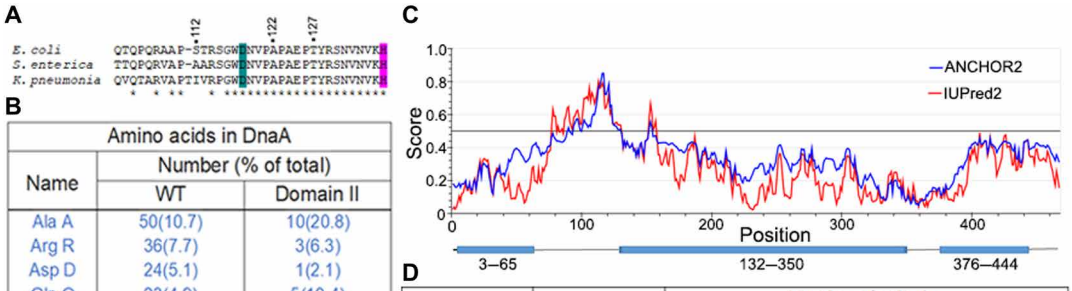

B

Amino acids in DnaA		
Name	Number (% of total)	
	WT	Domain II
Ala A	50(10.7)	10(20.8)
Arg R	36(7.7)	3(6.3)
Asp D	24(5.1)	1(2.1)
Gln Q	23(4.9)	5(10.4)
Ser S	24(5.1)	4(8.3)
Pro P	21(4.5)	7(14.6)
Trp W	5(1.1)	1(2.1)
Phe F	21(4.5)	None
Tyr Y	11(2.4)	1(2.1)
Ile I	23(4.9)	None
Leu L	48(10.3)	None
Cys C	3(0.6)	None
Met M	8(1.7)	None
Val V	30(6.4)	6(12.5)
Asn N	29(6.2)	4(8.3)
Thr T	25(5.4)	4(8.3)
Gly G	23(4.9)	1(2.1)
His H	9(1.9)	None
Lys K	23(4.9)	None
Glu E	31(6.6)	1(2.1)

D

E. coli HDL1001 with	DnaA	Number of colonies			
		IPTG, 1 mM	No IPTG		
			Ara, 0.2%	Glu, 0.2%	
pBAD	None	1000	<1	<1	<1
pZL606	WT	1000	<1	<1	<1
pSR1	DnaAΔ87–134	1000	<1	<1	<1
pSR2	DnaAΔ87–91	1000	<1	<1	<1
pSR3	DnaAΔ92–96	1000	<1	<1	<1
pSR4	DnaAΔ97–101	1000	<1	<1	<1
pSR5	DnaAΔ102–106	1000	<1	<1	<1
pSR6	DnaAΔ107–112	1000	<1	<1	<1
pSR7	DnaAΔ112–116	1000	<1	832 ± 228	<1
pSR8	DnaAΔ117–121	1000	<1	<1	<1
pSR9	DnaA Δ122–126	1000	<1	1030 ± 234	<1
pSR10	DnaAΔ127–131	1000	<1	905 ± 218	<1
pSR11	DnaAΔ131–134	1000	<1	<1	<1
pZL607	DnaAL366K	1000	<1	802 ± 172	<1
pRS19	DnaAD118Q	1000	<1	<1	<1

Fig. 5. The short deletions in the DnaA linker region flanking D118 suppress the requirement of anionic phospholipids for cellular growth. (**A**) *E. coli* DnaA domain II is intrinsically disordered. Multiple-sequence alignment of DnaA homologs from γ-proteobacteria (*E. coli*, *S. enterica*, and *K. pneumonia*) revealed 100% identity in the distal half (Gly^{115}-His^{136}) of unstructured linker domain. (**B**) Comparative analysis of amino acid composition of full-length DnaA versus linker domain. Hydrophilic and hydrophobic amino acid residues are indicated by blue and red colors. (**C**) Analysis of *E. coli* DnaA using ANCHOR2 (indicated in blue) and IUPred2 (indicated in red) tools predicted IDRs residing between amino acid residues 66 to 131 and 351 to 375. (**D**) Removal of specific short linear motifs in linker region (first amino acid of each short sequence is indicated by number on the top of sequence alignment) suppresses the growth arrest of acidic phospholipid–deficient *E. coli* cells. *E. coli* cells containing chromosomal copy of *pgs*A gene under IPTG-inducible promoter are transformed with *dnaA* deletion mutants cloned under arabinose-inducible promoter and plated on LB-agar plates with 1 mM IPTG and appropriate antibiotics. The cells containing each mutant plasmid were grown until OD_{600} reached 0.1 and serially diluted to plate approximately 300 to 500 cells in medium containing 0 or 0.2% arabinose. The cells plated on LB agar containing 1 mM IPTG served as positive control and 0.2% glucose as negative control. The plates were incubated at 37°C. Colony numbers were after normalization to 1000 per plate.

further when 100 μM SUV was added (Fig. 7E). In contrast, at 25 μM SUV, melting points of DnaA(ΔS112-G116), DnaA(ΔA122-P126), and DnaA(ΔT127-N131) proteins did not exhibit any shift; the primary melting peak remained at 57°C (Fig. 7D). At 100 μM SUV, we noticed no change in the melting peak for DnaA(ΔS112-G116) and DnaA(ΔT127-N131) and a slight lowering in the melting point for DnaA(ΔA122-P126) (from 57° to 52°C) (Fig. 7E). No changes were found in the melting point of either the WT or any mutant DnaA protein when mixed with SUVs made up of 100 μM DOPC (1,2-dioleoyl-*sn*-glycero-3-phosphocholine) (Fig. 7F), which agree with the previous studies indicating that zwitterionic DOPC does not cause release of ATP bound to DnaA (*41*). These results were also confirmed by filter retention assay that measures radiolabeled ATP bound to DnaA (fig. S12). ATP release was evident only for the WT and, to a lesser extent, for the L366K mutant in the presence of anionic PG and not zwitterionic PC. The inability of PG to release ATP from the deletion mutants suggests that the deleted regions in the linker are involved in interaction with anionic phospholipids present in the *E. coli* membrane.

DISCUSSION

In multidomain proteins, which are common across biology, the domains often are connected with unstructured linkers of various lengths (typically between 5 and 40 amino acid residues). Increasing knowledge of protein structure and function relationship suggests that flexible linkers may play important roles in protein function, in addition to their basic role in joining flanking structured domains (*54*). The initiator protein for *E. coli* chromosomal replication, DnaA, has four domains (I to IV), of which three (I, III, and IV) are relatively rigid with distinct but mutually dependent roles. In contrast, domain II is considered flexible, and other than linking domains I and III, there is scant evidence of its more direct role in DnaA functions. Here, we find that certain changes in the linker region can affect functions as fundamental as ATP binding, a function normally attributed to the well conserved (AAA+) domain III of DnaA. Moreover, some different changes in the linker region allow cells to bypass the requirement of acidic membranes for cellular growth, which suggests a second role for the linker region possibly in membrane-related unbinding of ATP from DnaA.

Contribution of the linker domain residue Asp^{118} in ATP binding

DnaA is a member of the AAA+ superfamily, and like other members, the amino acid residues forming the adenine nucleotide–binding pocket primarily reside in the conserved motifs, such as DnaA's Walker A (Lys^{178}) and Walker B motifs (Asp^{235}) (*8*). A wealth of knowledge obtained from genetic and biochemical studies indicates

A

Amino acid change	ATP-binding stoichiometry (fmol ATP/fmol protein)	K_d (ATP binding) (μM)
DnaA(WT)	0.31 ± 0.02	0.15 ± 0.02
DnaA(Δ112–116)	0.15 ± 0.03	0.10 ± 0.02
DnaA(Δ122–126)	0.16 ± 0.05	0.19 ± 0.03
DnaA(Δ127–131)	0.20 ± 0.04	0.08 ± 0.01
DnaA(L366K)	0.30 ± 0.04	0.11 ± 0.04
DnaA(Δ87–134)	0.03 ± 0.02	3.08 ± 0.72

B

E. coli CM742 with	Relative number of colonies (30°C)		
	0 Ara/Glu	0.2% Ara	0.2% Glu
pBAD	1000	1137 ± 213	1154 ± 103
p*dnaA*	1000	1191 ± 155	1036 ± 108
p*dnaA*Δ112–116	1000	1126 ± 195	1017 ± 129
p*dnaA*Δ122–126	1000	1120 ± 174	1104 ± 108
p*dnaA*Δ127–131	1000	1030 ± 204	1077 ± 172

C

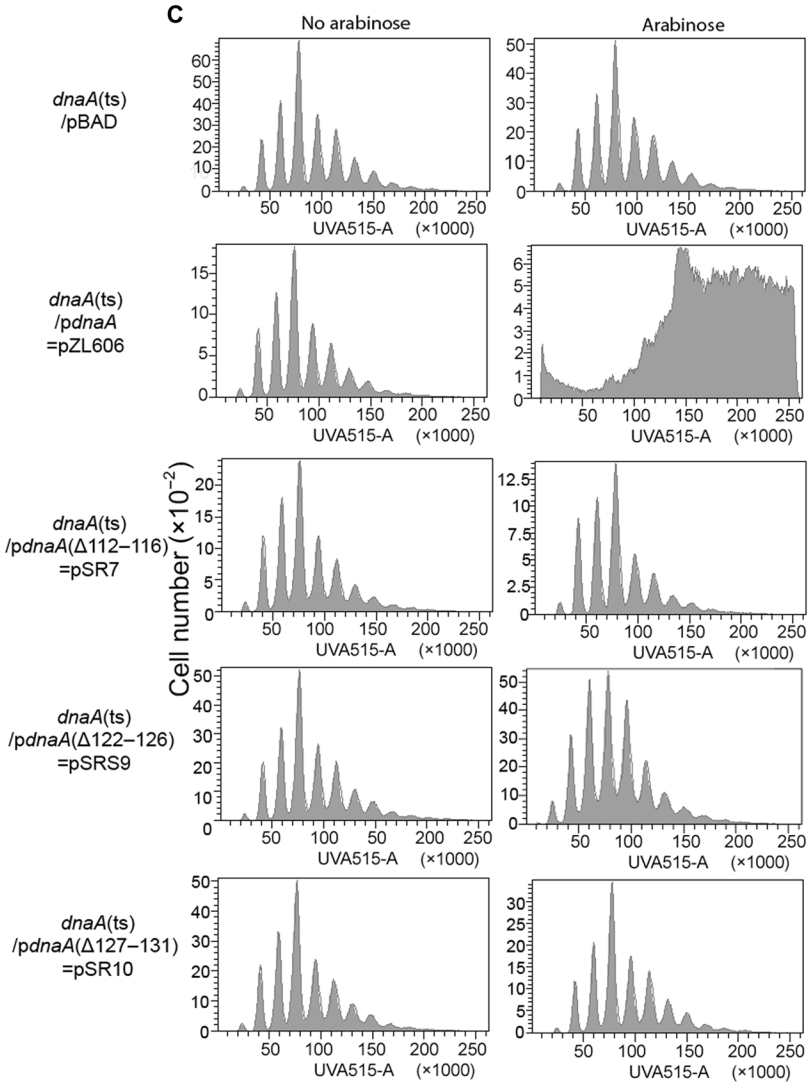

Fig. 6. DnaA with small deletions in linker retains high affinity for ATP binding and does not compromise *dnaA46*(ts) growth at permissive temperature. (**A**) WT and mutant proteins (0.15 to 0.9 μM) were incubated with 1 μM [α-32]-ATP, and nucleotide binding was measured by filter retention assay (*41*). WT and mutant proteins (1.9 μM) were incubated with [α-32]-ATP (range between 0.005 and 2.5 μM) for 15 min at 4°C to calculate K_d values. Nucleotide binding was measured by filter retention assay. Mean (±SD) values represent data from three independent sets of experiments. (**B**) *E. coli* CM742 (=*dnaA46*ts) cells transformed with pBAD vector, pZL606 carrying *dnaA*(WT) and its derivatives pRS7 carrying *dnaA*(Δ112–116), pRS9 carrying *dnaA*(Δ122–126), and pRS10 carrying *dnaA*(Δ127–131) cloned under arabinose-inducible promoter and plated on LB-agar plates containing ampicillin and streptomycin. Single transformants obtained on plates were grown to an OD_{600} of ~0.1, and after appropriate dilution (~1000-fold), cells (100 μl) were plated on LB-agar plates supplemented with 0.2% arabinose. Plates were incubated at 30°C for 16 to 24 hours. Cells plated on LB-agar plates containing no arabinose or 0.2% glucose served as control. To calculate transformation efficiencies, colony numbers were normalized to 1000 for growth in the presence of no inducer at 30°C. Data represent average values from at least three biological replicates. (**C**) *E. coli* CM742 cells were transformed with vector pBAD and its derivatives pZL606 carrying *dnaA*(WT), pRS7 carrying *dnaA*(Δ112–116), pRS9 carrying *dnaA*(Δ122–126), and pRS10 carrying *dnaA*(Δ127–131) expressing WT or mutant DnaA proteins from an arabinose-inducible promoter. Otherwise, the details are the same as in Fig. 3.

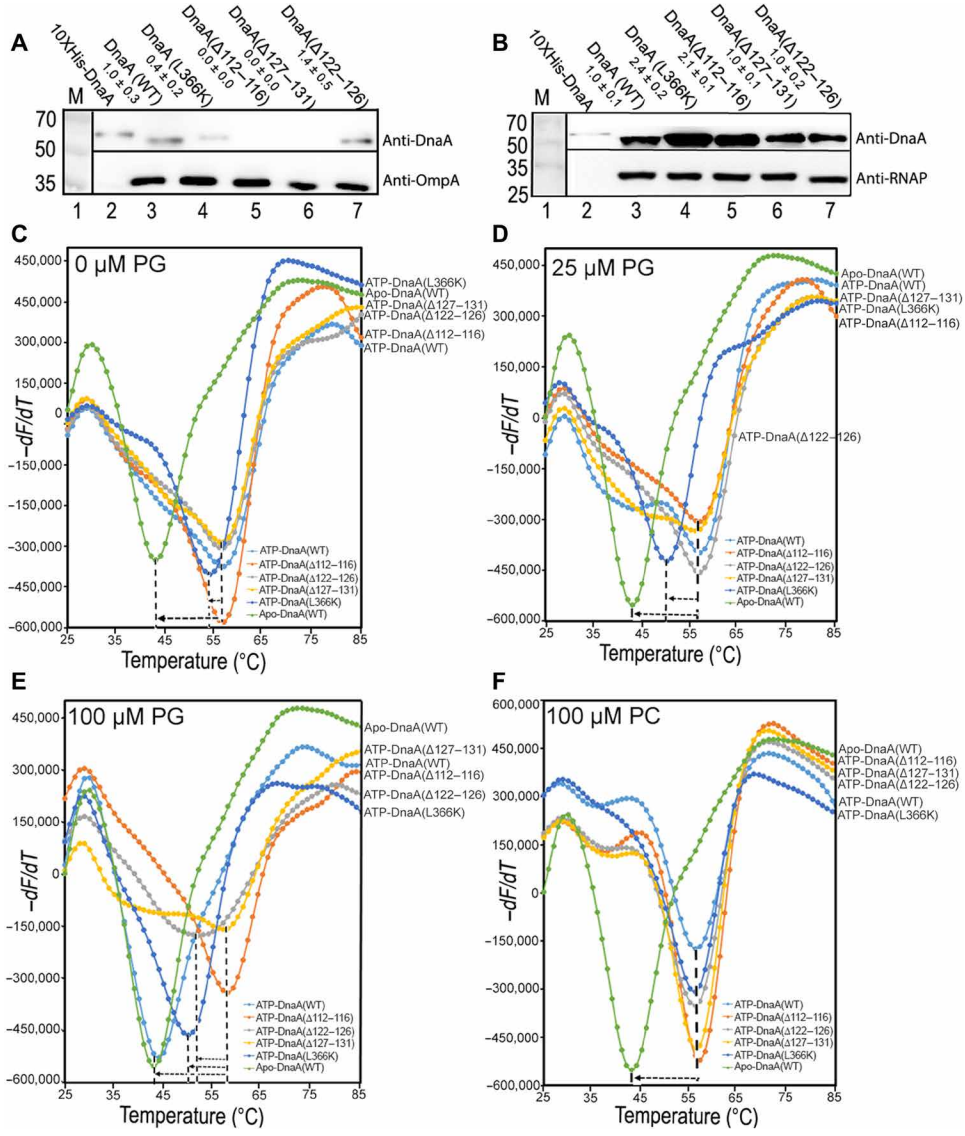

Fig. 7. The short deletions in the DnaA linker region alter their interactions with anionic phospholipids. (**A**) EH3287 (=Δ*dnaA*/*pgsA*$^+$) cells, transformed with plasmids carrying WT and mutant *dnaA* alleles under arabinose-inducible promoter, were grown to an OD_{600} of ~0.1, and *dnaA* expression was induced by inclusion of 0.2% arabinose for 90 min. Cells were processed to separate the cytosolic and membrane-bound proteins as discussed in Materials and Methods. Two micrograms of total protein in each lane (lanes 3 to 7) was resolved on 12% SDS-PAGE and transferred to polyvinylidene difluoride membranes for immunoblotting using polyclonal anti-DNA antibody. 10X His-tagged DnaA (lane 2) was used as a positive control. Representative gels are presented here to show the distribution of WT and mutant DnaA proteins present in the cytosolic (**A**) and detergent-solubilized fractions (**B**). *E. coli* outer membrane protein A (ompA) protein (for membrane-solubilized fractions, 35 kDa) and RNA polymerase (RNAP) protein (for cytosolic fraction, 28 kDa) were used as loading controls, and they were detected using anti-OmpA and α-subunit of anti-RNAP antibodies. Relative to WT, the mutant DnaA protein amount (average ± SD from three biological replicates) is indicated below each mutant name in the top. M indicates the molecular weight of proteins in kilodaltons. (**C** to **F**) WT and mutant DnaA proteins (10 μM) mixed with ATP (5 mM) and incubated in ice for 15 min in a 96-well plate. SUVs composed of purified PG or PC were included at the indicated concentrations. Following addition of 3 μl of SYPRO Orange dye (at 50× dilution in water), the fluorescence data were collected between 25° and 95°C with the temperature gradient set for 1 min/°. T_m and *−dF/dT* values were calculated by fitting the data to sigmoidal dose-response (variable slope) equation using the GraphPad Prism software.

that amino acid residues such as Ala^{184} (*22*), Ala^{213} (*55*), and Glu^{143} (*56*) that lie outside of these motifs are also critical for ATP binding, and mapping of these residues on a high-resolution x-ray crystal structure of truncated *A. aeolicus* DnaA supports this concept. However, the lack of structural information on any full-length DnaA leaves open the possibility that allosteric interdomain communication might also be important for ATP-binding activity of DnaA. Our previous study that used limited proteolysis with trypsin and chymotrypsin identified sites of protease susceptibility that differ between ATP-DnaA and ADP-DnaA (*34*). The sites largely reside in the amino terminal half of DnaA, including the linker region (*34*).

Here, using a structure-guided full-length *E. coli* DnaA model, we identified that the residues Asp^{118} and His^{136} might be linked to each other by hydrogen bond interactions (predicted distance between the two residues is 3.0 A) (Fig. 1B and fig. S3A). We note that in our model (Fig. 1B and PDB 1L8Q), a water molecule is predicted

to be in close proximity to Asp[118] and His[136], which is known to interact with the hydroxyl oxygen of ribose carbon at C3 position of ATP (*5*). We speculate that in nucleotide-free DnaA, the loop region carrying Asp[118] remains in an open configuration, but when bound to the adenine nucleotide the loop region comes into close proximity to AAA+ domain, establishing a proton relay using the water molecule that could act as a nucleophilic center (Fig. 8). The proton relay would cause deprotonation of Asp[118], assisting in stable ATP binding by closing the loop. Simultaneously, the proton relay may also cause protonation at the imidazole group of His[136], which is required

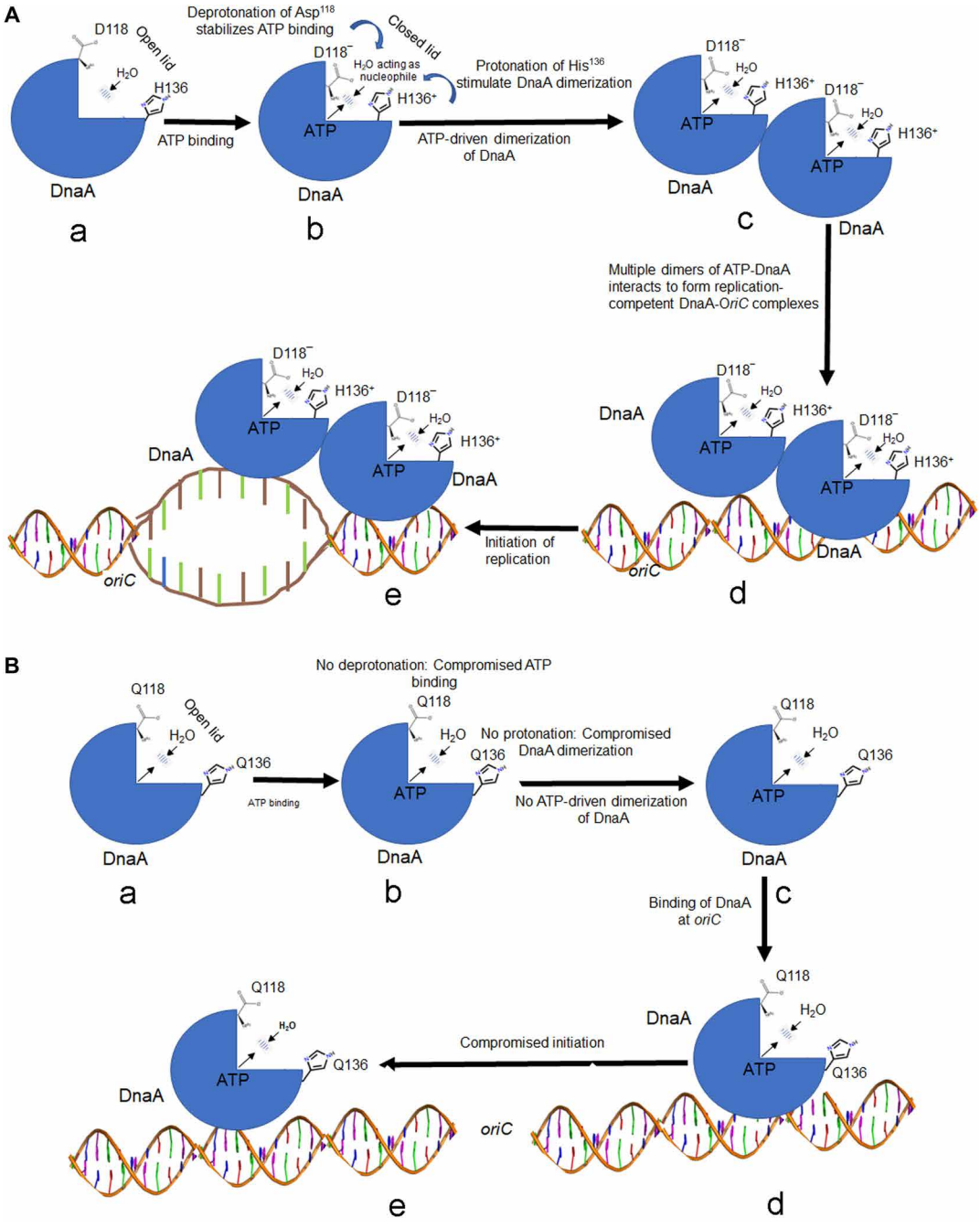

Fig. 8. Schematic diagram on how Asp[118] and His[136] could be involved in ATP-dependent DnaA oligomerization. (**A**) A flexible loop in DnaA containing Asp[118] and His[136] in an open-loop confirmation undergoes local rearrangements in the presence of the cellular levels of ATP that initiates a proton relay from the water molecule (possibly acting as a nucleophile) present near the nucleotide-binding pocket (a). Such changes might promote deprotonation of Asp[118] required for ATP binding (b). The released proton protonates imidazole present in His[136] (II), which is important for DnaA dimer formation (c). This makes DnaA replication competent at the chromosomal *oriC* (d) by opening the duplex DNA (e) (*5*). (**B**) The presence of Glu(Q) at Asp[118] position (a) abrogates ATP binding (b) and thus fails to form DnaA dimer (c) required to make *oriC* replication competent (d) and open (e). The presence of Glu(Q) at His[136], although does not cause significant reduction in ATP binding, does abrogate DnaA dimerization (*5*).

for DnaA dimerization and making *oriC* competent for replication (*5*, Fig. 8). The presence of Gln at either Asp^{118} (in the present study) or His^{136} (*5*) affects ATP-mediated DnaA oligomerization, possibly by interfering with the proton relay due to its neutral charge. In contrast, substitution of Asp^{118} with Ala (fig. S3B) or His^{136} with Ala in our previous study (*5*) may result in the loss of Asp^{118}-His^{136} hydrogen bond but allow water to occupy the vacated space. This might cause a solvated transition state, allowing the protein to function in the proton relay.

We predict that the activity of DnaA protein might be allosterically controlled by local deprotonation and protonation of Asp^{118} and His^{136} residues that drive dynamic changes in the functional states of the protein (Fig. 8). The possibility cannot be excluded that ATP binding in the nucleotide-binding pocket causes disorder-to-order transitions of the linker region that drive the protonation-deprotonation changes. We would like to note here that systematic deletions in *E. coli dnaA* that result in shortened DnaA domain II are allowed without affecting cell viability (*57*). For example, *E. coli* DnaA lacking amino acid residues 96 to 120 in the linker region supports cell growth and retains its ability to bind the ATP (*15*). We believe that DnaA lacking a region that contains D118, such as for DnaA (Δ96–120), may still be able to stably bind ATP because the resulting vacant space occupied by water molecules keeps the proton relay intact. It appears that the presence of Asp^{118} residue is not essential for DnaA ATP binding, but it may play a role in stabilizing ATP-DnaA complex.

We find that the overexpression of DnaA(D118Q) cannot be tolerated in *dnaA46*ts strain at low temperatures (Table 2). Like DnaA(A184V), the growth restriction of *dnaA46*ts cells overexpressing DnaA(D118Q) could be attributed to its ATP-binding defect. As shown in our homology model, a loop carrying Asp^{118} might interact with the nucleotide-binding pocket, primarily through Ala^{184} (Fig. 1B), and the replacement of the Asp^{118} with Gln^{118} resulted in destabilizing the nucleotide-binding pocket. This could be the main reason why both DnaA(D118Q) and DnaA(A184V) showed similar temperature-dependent growth properties.

Short deletions in the linker alter the ability of DnaA protein to interact with membranes

Membrane association has been probed by two assays here. When subcellular fractions were examined, we found that of the three DnaA mutants carrying short deletions that allowed cell growth without PG, two DnaA(Δ112–116) and DnaA(Δ127–131) were completely defective in membrane binding by DnaA. Another deletion mutant DnaA(Δ122–126) retained the binding activity, similar to DnaA(WT) (Fig. 7A). The membrane association was probed also with ThermoFluor assay for protein thermostability. The premise here is that DnaA that gains thermostability upon interaction with ATP would become unstable if interactions with PG release the bound ATP. By this assay, all the three deletion mutants discussed above remained thermoresistant in the presence of PG, indicating that they did not interact with the anionic membrane effectively (Fig. 7, C to E). Overall, the two assays support the notion that specific short stretches in the linker interact with PG of the inner cell membrane possibly to activate DnaA-ADP by releasing the nucleotide. The deletion of those stretches can achieve the allosteric change required for DnaA activation without the presence of PG. Previous studies have shown that defective growth of Δ*pgsA* cells are suppressed by overexpression of DnaA containing deletions in domain III (AAA+ ATPase domain) or in domain IV (DNA binding domain) (*40*). Now, we show the same for domain II. The change in domain IV may appear unexpected, but two DNA sites, *datA* (*30*) and DARS (*33*), involved in controlling DnaA-ATP level depend on DnaA binding to specific sites within them. The widespread occurrence of suppressors of Δ*pgsA* perhaps suggests that practically the entire protein is amenable to allosteric remodeling necessary for lipid dependent rejuvenation of DnaA to the initiator form, ATP-DNA. Some of these changes could be bypass mutations also, but how they are functioning needs to be understood. We note that the present results and those of others (*35*, *36*, *40*, *58*) are contradicted by a recent report that shows that down-regulation of *pgsA* does not perturb replication initiation (*59*). This discrepancy remains to be resolved.

In summary, the present study provides evidence that the linker domain of DnaA can play a significant role in ATP binding and membrane association, functions which were so far thought to be exclusive to the AAA+ domain. Considering that DnaA is a key regulator of initiation in *E. coli*, in-depth studies of mutant variants are required to understand regulation of replication initiation. The relevance of our work may also extend beyond bacteria as the presence of an IDR was shown in the aminoterminal of eukaryotic initiators ORC, Cdc6, and Cdt1, and the role of IDRs is shown to regulate multiple functions, including chromosome recruitment, initiator-specific coassembly, and Mcm2-7 helicase loading (*60*).

MATERIALS AND METHODS

Bacterial strains and plasmids

E. coli strains and plasmids used in this study are described in tables S1 and S2, respectively. Deoxyribo-oligonucleotides used in the study were commercially synthesized by Integrated DNA Technologies Inc. The list of DNA oligos is provided in table S3.

Site-directed mutagenesis and construction of plasmids containing mutated *dnaA* genes

A polymerase chain reaction (PCR)–based site-directed mutagenesis technique was used to introduce mutations in the *dnaA* gene of pZL411 (*41*). For each mutation, we used two external primers (CR4 and CR30), each containing the sites for Nde I or Bam HI, and two internal primers containing the desired base changes within the *dnaA* gene (table S3). Subsequently, two sets of primary (using pZL411 as the template) and one set of secondary PCR amplifications (using the mixture of primary amplification products as the template) were carried out with T4 DNA polymerase. The amplified products were digested with restriction enzymes Nde I and Bam HI and incorporated between same restriction sites of pZL411 plasmid (*41*) to generate plasmids pRS15 (carrying *dnaA*D118A), pRS16 (carrying *dnaA*D118Q), and pRS17 (carrying *dnaA*A184V) (table S2). The presence of mutations was confirmed by DNA sequencing. The mutant *dnaA* genes were also cloned under an arabinose-inducible promoter between Nde I and Hind III restriction sites as is the case for the WT *dnaA* gene of plasmid pZL606 (*40*). This created isogenic plasmids pRS18 (carrying *dnaA*D118A), pRS19 (carrying *dnaA*D118Q), and pRS20 (carrying *dnaA*A184V) (table S2). Plasmid pRD was generated by cloning a fragment carrying *seqA* allele under P*lac* promoter between Sca I and Eco RI sites of plasmid pACYC encoding tetracycline resistance gene and p15A origin of replication (*50*).

Homology modeling

The truncated structures of domains I and II (amino acid residues 1 to 139) based on the structure of *E. coli* DnaA [PDB ID: 2E0G carrying residues 1 to 108; (*43*)] and domains III and IV (amino acid residues 134 to 467) based on the structure of *A. aeolicus* DnaA [PDB ID: 1L8Q; (*9*)] as template were generated using Phyre2 server (*44*). A full-length *E. coli* DnaA structure was constructed by merging the two truncated structures together using Coot software (*45*), and the model was energy-minimized using Amber software (*46*). A model that had satisfied geometrical constraints as evident from Ramachandran plot was chosen to add ATP using Coot, on the basis of the structural restraints of AMPPCP binding in *A. aeolicus* DnaA [PDB ID: 2HCB; (*10*)]. The entire structure was again energy-minimized using the Amber software (*48*) in the flexible docking mode allowing movement of the linker domain.

Protein expression and purification

Overexpression and purification of NH_2-terminally 10× histidine-tagged proteins were performed as described previously (*41*). Briefly, *E. coli* BL21 (DE3LysS) cells (Stratagene) were transformed with pZL411 plasmids containing WT *dnaA* and pRS15-pRS17 containing mutant derivatives of *dnaA*. The transformants were grown to an OD_{600} of 0.6 to 0.8, and *dnaA* expression was induced by inclusion of 1 mM IPTG. The growth was continued for an additional 90 min. Cells were harvested by centrifugation (at 6000 rpm for 15 min) and suspended in native binding buffer [50 mM sodium phosphate (pH 7.5), 500 mM NaCl, and 5 mM imidazole], and proteins were extracted and purified as described earlier (*41*). The purity of the proteins was analyzed in a 12% SDS-PAGE, and protein amounts were quantified using the Bradford assay. Protein samples were aliquoted and stored at −80°C until further use.

Nucleotide-binding assay

Filter binding assays were performed as described earlier (*41*). Briefly, DnaA protein (140 to 840 ng) was incubated with 1 μM [α-32]-ATP in PP-60 buffer [50 mM Hepes-KOH (pH7.6) at 1 M, 2.5 mM magnesium acetate, 20% (v/v) glycerol, 0.007% (v/v) Triton X-100, 0.3 mM EDTA, and 7 mM dithiothreitol] for 15 min at 4°C. To calculate dissociation constant, proteins (2.5 pmol) were incubated with 32P-αATP (range between 0.005 and 2.5 μM) in PP-60 buffer for 15 min at 4°C. To assess the stability of nucleotide binding, WT and mutant DnaA proteins were incubated with 1 μM [α-32]-ATP at 4°, 30°, and 42°C for different time intervals. Reaction mixtures were filtered through a nitrocellulose membrane filter (presoaked in a wash buffer) and dried under a lamp, and the radioactivity retained was measured by liquid scintillation counting.

ThermoFluor assay

Purified WT and mutant DnaA proteins mixed with ATP (5 mM) in a 96-well PCR plate (MicroAmp Fast 96-Well Reaction Plate, 0.1 ml) were incubated on ice for 15 min. Reactions were set up in the absence or presence of SUVs composed of DOPG or DOPC. Following the addition of 3 μl of SYPRO Orange dye (50× diluted in water) in each well (final volume of 50 μl), fluorescence data were collected on the Applied Biosystems Real-Time PCR Instrument System using the StepOne software v2.3. The temperature was set to increase in gradient at 1 min/° from 25° to 95°C. Melting temperature (T_m) and differential fluorescence ($-dF/dT$) values were calculated by fitting the data on sigmoidal dose-response (variable slope) equation in GraphPad Prism software.

In vivo replication assay

E. coli EH3827 cells [kanamycin resistant; (*48*)] were transformed with plasmids containing *dnaA* or its mutant derivatives, pRS18-pRS20 (ampicillin resistant; table S2), and the transformants were further transformed with the *oriC* plasmid pAL70 [p*oriC*, chloramphenicol resistant; (*5*)]. The transformation mixtures were plated at LB-agar plates with and without selection for the p*oriC* plasmid and in the absence or presence of the inducer arabinose (0.05, 0.1, and 0.2%), and plates were subsequently incubated at 37°C for 16 to 24 hours. Colony numbers were recorded and averaged from at least three biological replicates.

Assay for temperature-sensitivity of growth

E. coli CM742 *dnaA46*ts was made competent and transformed with plasmids carrying the *dnaA* gene and its mutant derivatives, pRS18 to pRS20 (table S2). The transformants were selected for growth at 30°C on LB-agar plates supplemented with streptomycin (50 μg/ml) and ampicillin (100 μg/ml). Single colonies inoculated in LB medium (supplemented with appropriate antibiotics) were grown to an OD_{600} of ~0.1. Equal OD units of culture (prepared by appropriate dilutions) were plated in replicas on LB-agar plates (containing appropriate antibiotics) in the absence or presence of 0.05, 0.1, and 0.2% arabinose and 0.2% glucose. The plates were incubated at 30° and 42°C, and colony counts were averaged from at least three biological replicates.

Cells carrying plasmid pRD (expressing SeqA) placed under P*lac* promoter grown in LB-agar supplemented with teracycline and 50 μM IPTG to make them competent (table S2). The SeqA-expressing plasmid, pRD, was a derivative of pACYC184 (*50*). The competent cells were transformed with DnaA-expressing plasmids, pRS18 to pRS20 (table S2). The transformants carrying plasmid pRD (carrying *seqA*) and pBAD alone or carrying *dnaA* (pRS18) or its derivative [*dnaA*D118Q (pRS19) and *dnaA*D118Q (pRS20)] were selected for growth at 30°C on LB-agar plates supplemented with tetracycline (12.5 μg/ml) and ampicillin (100 μg/ml). Single colonies inoculated in LB medium (supplemented with appropriate antibiotics) were grown to an OD_{600} of ~0.1. Equal OD units of culture (prepared by appropriate dilutions) were plated in replicas on LB-agar plates (containing appropriate antibiotics) in the absence or presence of 0.2% arabinose and 0.2% glucose.

Flow cytometry

Overnight grown cell cultures were diluted to an OD_{600} of ~0.005 in fresh LB medium supplemented with appropriate antibiotics. The cultures were grown for 45 min and then divided into two equal volumes and to one of which arabinose was added to 0.2% to induce the expression of different *dnaA* alleles. Cells were further grown up to an OD_{600} of 0.15 and then treated with rifampicin (150 μg/ml) and cephalexin (10 μg/ml) to inhibit new rounds of replication initiation and cell division, respectively, and were grown for additional 2.5 hours to allow time for completion of ongoing rounds of replication (*20*). The cells were analyzed for DNA contents using a BD LSRFortessa SORP flow cytometer.

Assay for anionic membrane requirement for growth

E. coli HDL1001 (*pgsA* null) cells were made competent and transformed with plasmids carrying the *dnaA* gene and its mutant derivatives, pSR1 to pSR11 (Fig. 5D). The transformants were selected for growth at 37°C on LB-agar plates supplemented with kanamycin

(50 μg/ml) and IPTG (1 mM). Single colonies were used to inoculate LB medium (supplemented with appropriate antibiotics and without IPTG), and the cultures were grown to an OD_{600} of ~0.1. Equal OD units of culture (prepared by appropriate dilutions) were plated on LB-agar plates (containing appropriate antibiotics) in the presence of IPTG (1 mM) or 0.2% arabinose or 0.2% glucose. The plates were incubated at 37°C, and colony counts were averaged from at least three biological replicates.

Subcellular fractionation

EH3287 (Δ*dnaA*/*pgsA*$^+$) cells carrying plasmids with WT or mutant *dnaA* alleles placed under arabinose-inducible promoter were grown to an OD_{600} of ~0.1. Protein expression was induced by adding 0.2% arabinose and subsequent growth for an additional 90 min. The cells were lysed with lysozyme (300 μg/ml) and freeze-thaw (three times). The cytosolic and membrane fractions were separated by centrifugation (44,000 rpm for 30 min). The membrane fraction was solubilized using anionic detergents, followed by high-speed centrifugation. The membrane-solubilized protein fractions were extensively dialyzed overnight (with three changes of buffer) to remove the anionic detergents. Two micrograms of total protein was loaded per lane and resolved in 12% SDS-PAGE. The protein bands were transferred to polyvinylidene difluoride membranes for immunodetection of DnaA protein.

SUPPLEMENTARY MATERIALS

Supplementary material for this article is available at https://science.org/doi/10.1126/sciadv.abq6657

View/request a protocol for this paper from *Bio-protocol*.

REFERENCES AND NOTES

1. H. Kawakami, T. Katayama, DnaA, ORC, and Cdc6: Similarity beyond the domains of life and diversity. *Biochem. Cell Biol.* **88**, 49–62 (2010).
2. M. D. Sutton, J. M. Kaguni, The *Escherichia coli* dnaA gene: Four functional domains. *J. Mol. Biol.* **274**, 546–561 (1997).
3. R. Saxena, N. Fingland, D. Patil, A. K. Sharma, E. Crooke, Crosstalk between DnaA protein, the initiator of *Escherichia coli* chromosomal replication, and acidic phospholipids present in bacterial membranes. *Int. J. Mol. Sci.* **14**, 8517–8537 (2013).
4. L. A. Simmons, M. Felczak, J. M. Kaguni, DnaA protein of *Escherichia coli*: Oligomerization at the *E. coli* chromosomal origin is required for initiation and involves specific N-terminal amino acids. *Mol. Microbiol.* **49**, 849–858 (2003).
5. R. Saxena, C. B. Stanley, P. Kumar, M. J. Cuneo, D. Patil, J. Jha, K. L. Weiss, D. K. Chattoraj, E. Crooke, A nucleotide-dependent oligomerization of the *Escherichia coli* replication initiator DnaA requires residue His^{136} for remodeling of the chromosomal origin. *Nucleic Acids Res.* **48**, 200–211 (2020).
6. M. D. Sutton, K. M. Carr, M. Vicente, J. M. Kaguni, *Escherichia coli* DnaA protein. The N-terminal domain and loading of DnaB helicase at the *E. coli* chromosomal origin. *J. Biol. Chem.* **273**, 34255–34262 (1998).
7. K. Keyamura, N. Fujikawa, T. Ishida, S. Ozaki, M. Su'etsugu, K. Fujimitsu, W. Kagawa, S. Yokoyama, H. Kurumizaka, T. Katayama, The interaction of DiaA and DnaA regulates the replication cycle in *E. coli* by directly promoting ATP DnaA-specific initiation complexes. *Genes Dev.* **21**, 2083–2099 (2007).
8. T. Mizushima, T. Takaki, T. Kubota, T. Tsuchiya, T. Miki, T. Katayama, K. Sekimizu, Site-directed mutational analysis for the ATP binding of DnaA protein. Functions of two conserved amino acids (Lys^{178} and Asp^{235}) located in the ATP-binding domain of DnaA protein in vitro and in vivo. *J. Biol. Chem.* **273**, 20847–20851 (1998).
9. J. P. Erzberger, M. M. Pirruccello, J. M. Berger, The structure of bacterial DnaA: Implications for general mechanisms underlying DNA replication initiation. *EMBO J.* **21**, 4763–4773 (2002).
10. J. P. Erzberger, M. L. Mott, J. M. Berger, Structural basis for ATP-dependent DnaA assembly and replication-origin remodeling. *Nat. Struct. Mol. Biol.* **13**, 676–683 (2006).
11. S. Nishida, K. Fujimitsu, K. Sekimizu, T. Ohmura, T. Ueda, T. Katayama, A nucleotide switch in the *Escherichia coli* DnaA protein initiates chromosomal replication: Evidence from a mutant DnaA protein defective in regulatory ATP hydrolysis in vitro and in vivo. *J. Biol. Chem.* **277**, 14986–14995 (2002).
12. J. Garner, E. Crooke, Membrane regulation of the chromosomal replication activity of *E. coli* DnaA requires a discrete site on the protein. *EMBO J.* **15**, 3477–3485 (1996).
13. J. Garner, P. Durrer, J. Kitchen, J. Brunner, E. Crooke, Membrane-mediated release of nucleotide from an initiator of chromosomal replication, *Escherichia coli* DnaA, occurs with insertion of a distinct region of the protein into the lipid bilayer. *J. Biol. Chem.* **273**, 5167–5173 (1998).
14. N. Fujikawa, H. Kurumizaka, O. Nureki, T. Terada, M. Shirouzu, T. Katayama, S. Yokoyama, Structural basis of replication origin recognition by the DnaA protein. *Nucleic Acids Res.* **31**, 2077–2086 (2003).
15. K. L. Molt, V. A. Sutera, K. K. Moore, S. T. Lovett, A role for nonessential domain II of initiator protein, DnaA, in replication control. *Genetics* **183**, 39–49 (2009).
16. R. S. Fuller, J. M. Kaguni, A. Kornberg, Enzymatic replication of the origin of the *Escherichia coli* chromosome. *Proc. Natl. Acad. Sci. U.S.A.* **78**, 7370–7374 (1981).
17. N. E. Dixon, A. Kornberg, Protein HU in the enzymatic replication of the chromosomal origin of *Escherichia coli*. *Proc. Natl. Acad. Sci. U.S.A.* **81**, 424–428 (1984).
18. D. Bramhill, A. Kornberg, Duplex opening by dnaA protein at novel sequences in initiation of replication at the origin of the *E. coli* chromosome. *Cell* **52**, 743–755 (1988).
19. E. Boye, A. Løbner-Olesen, K. Skarstad, Timing of chromosomal replication in *Escherichia coli*. *Biochim. Biophys. Acta* **951**, 359–364 (1988).
20. K. Skarstad, K. von Meyenburg, F. G. Hansen, E. Boye, Coordination of chromosome replication initiation in *Escherichia coli*: effects of different dnaA alleles. *J. Bacteriol.* **170**, 852–858 (1988).
21. T. R. Hupp, J. M. Kaguni, DnaA5 protein is thermolabile in initiation of replication from the chromosomal origin of *Escherichia coli*. *J. Biol. Chem.* **268**, 13128–13136 (1993).
22. K. M. Carr, J. M. Kaguni, The A184V missense mutation of the dnaA5 and dnaA46 alleles confers a defect in ATP binding and thermolability in initiation of *Escherichia coli* DNA replication. *Mol. Microbiol.* **20**, 1307–1318 (1996).
23. G. Kellenberger-Gujer, A. J. Podhajska, L. Caro, A cold sensitive dnaA mutant of *E. coli* which overinitiates chromosome replication at low temperature. *Mol. Gen. Genet.* **162**, 9–16 (1978).
24. T. Katayama, A. Kornberg, Hyperactive initiation of chromosomal replication in vivo and in vitro by a mutant initiator protein, DnaAcos, of *Escherichia coli*. *J. Biol. Chem.* **269**, 12698–12703 (1994).
25. R. E. Braun, K. O'Day, A. Wright, Cloning and characterization of dnaA(Cs), a mutation which leads to overinitiation of DNA replication in *Escherichia coli* K-12. *J. Bacteriol.* **169**, 3898–3903 (1987).
26. M. Lu, J. L. Campbell, E. Boye, N. Kleckner, SeqA: A negative modulator of replication initiation in E. coli. *Cell* **77**, 413–426 (1994).
27. L. A. Simmons, J. M. Kaguni, The DnaAcos allele of *Escherichia coli*: Hyperactive initiation is caused by substitution of A184V and Y271H, resulting in defective ATP binding and aberrant DNA replication control. *Mol. Microbiol.* **47**, 755–765 (2003).
28. M. Nyborg, T. Atlung, O. Skovgaard, F. G. Hansen, Two types of cold sensitivity associated with the A184→V change in the DnaA protein. *Mol. Microbiol.* **35**, 1202–1210 (2000).
29. T. Mizushima, S. Nishida, K. Kurokawa, T. Katayama, T. Miki, K. Sekimizu, Negative control of DNA replication by hydrolysis of ATP bound to DnaA protein, the initiator of chromosomal DNA replication in *Escherichia coli*. *EMBO J.* **16**, 3724–3730 (1997).
30. T. Katayama, K. Fujimitsu, T. Ogawa, Multiple pathways regulating DnaA function in *Escherichia coli*: Distinct roles for DnaA titration by the datA locus and the regulatory inactivation of DnaA. *Biochimie* **83**, 13–17 (2001).
31. K. Sekimizu, A. Kornberg, Cardiolipin activation of dnaA protein, the initiation protein of replication in *Escherichia coli*. *J. Biol. Chem.* **263**, 7131–7135 (1988).
32. B. Y. Yung, A. Kornberg, Membrane attachment activates dnaA protein, the initiation protein of chromosome replication in *Escherichia coli*. *Proc. Natl. Acad. Sci. U.S.A.* **85**, 7202–7205 (1988).
33. K. Fujimitsu, T. Senriuchi, T. Katayama, Specific genomic sequences of *E. coli* promote replicational initiation by directly reactivating ADP-DnaA. *Genes Dev.* **23**, 1221–1233 (2009).
34. R. Saxena, S. Vasudevan, D. Patil, N. Ashoura, J. Grimwade, E. Crooke, Nucleotide-induced conformational changes in *Escherichia coli* DnaA protein are required for bacterial ORC to Pre-RC conversion at the chromosomal origin. *Int. J. Mol. Sci.* **16**, 27897–27911 (2015).
35. G. Newman, E. Crooke, DnaA, the initiator of *Escherichia coli* chromosomal replication, is located at the cell membrane. *J. Bacteriol.* **182**, 2604–2610 (2000).
36. K. Boeneman, S. Fossum, Y. Yang, N. Fingland, K. Skarstad, E. Crooke, *Escherichia coli* DnaA forms helical structures along the longitudinal cell axis distinct from MreB filaments. *Mol. Microbiol.* **72**, 645–657 (2009).
37. T. Regev, N. Myers, R. Zarivach, I. Fishov, Association of the chromosome replication initiator DnaA with the *Escherichia coli* inner membrane in vivo: Quantity and mode of binding. *PLOS ONE* **7**, e36441 (2012).
38. W. Xia, W. Dowhan, In vivo evidence for the involvement of anionic phospholipids in initiation of DNA replication in *Escherichia coli*. *Proc. Natl. Acad. Sci. U.S.A.* **92**, 783–787 (1995).

39. N. Fingland, I. Flåtten, C. D. Downey, S. Fossum-Raunehaug, K. Skarstad, E. Crooke, Depletion of acidic phospholipids influences chromosomal replication in *Escherichia coli*. *Microbiology* **1**, 450–466 (2012).
40. W. Zheng, Z. Li, K. Skarstad, E. Crooke, Mutations in DnaA protein suppress the growth arrest of acidic phospholipid-deficient *Escherichia coli* cells. *EMBO J.* **20**, 1164–1172 (2001).
41. Z. Li, J. L. Kitchen, K. Boeneman, P. Anand, E. Crooke, Restoration of growth to acidic phospholipid-deficient cells by DnaA(L366K) is independent of its capacity for nucleotide binding and exchange and requires DnaA. *J. Biol. Chem.* **280**, 9796–9801 (2005).
42. R. Saxena, T. Rozgaja, J. Grimwade, E. Crooke, Remodeling of nucleoprotein complexes is independent of the nucleotide state of a mutant AAA^+ protein. *J. Biol. Chem.* **286**, 33770–33777 (2011).
43. Y. Abe, T. Jo, Y. Matsuda, C. Matsunaga, T. Katayama, T. Ueda, Structure and function of DnaA N-terminal domains: specific sites and mechanisms in inter-DnaA interaction and in DnaB helicase loading on oriC. *J. Biol. Chem.* **282**, 17816–17827 (2007).
44. L. A. Kelley, S. Mezulis, C. M. Yates, M. N. Wass, M. J. Sternberg, The Phyre2 web portal for protein modeling, prediction and analysis. *Nat. Protoc.* **10**, 845–858 (2015).
45. P. Emsley, B. Lohkamp, W. G. Scott, K. Cowtan, Features and development of Coot. *Acta Crystallogr. D Biol. Crystallogr.* **66**, 486–501 (2010).
46. Y. Duan, C. Wu, S. Chowdhury, M. C. Lee, G. Xiong, W. Zhang, R. Yang, P. Cieplak, R. Luo, T. Lee, J. Caldwell, J. Wang, P. Kollman, A point-charge force field for molecular mechanics simulations of proteins based on condensed-phase quantum mechanical calculations. *J. Comput. Chem.* **24**, 1999–2012 (2003).
47. M. A. Larkin, G. Blackshields, N. P. Brown, R. Chenna, P. A. McGettigan, H. McWilliam, F. Valentin, I. M. Wallace, A. Wilm, R. Lopez, J. D. Thompson, T. J. Gibson, D. G. Higgins, Clustal W and Clustal X version 2.0. *Bioinformatics* **23**, 2947–2948 (2007).
48. E. B. Hansen, M. B. Yarmolinsky, Host participation in plasmid maintenance: Dependence upon DnaA of replicons derived from P1 and F. *Proc. Natl. Acad. Sci. U.S.A.* **83**, 4423–4427 (1986).
49. R. Schleif, AraC protein, regulation of the l-arabinose operon in *Escherichia coli*, and the light switch mechanism of AraC action. *FEMS Microbiol. Rev.* **34**, 779–796 (2010).
50. A. C. Chang, S. N. Cohen, Construction and characterization of amplifiable multicopy DNA cloning vehicles derived from the P15A cryptic miniplasmid. *J. Bacteriol.* **134**, 1141–1156 (1978).
51. B. Mészáros, G. Erdos, Z. Dosztányi, IUPred2A: Context-dependent prediction of protein disorder as a function of redox state and protein binding. *Nucleic Acids Res.* **46**, W329–W337 (2018).
52. V. N. Uversky, Intrinsically disordered proteins from A to Z. *Int. J. Biochem. Cell Biol.* **43**, 1090–1103 (2011).
53. Z. Dosztányi, B. Mészáros, I. Simon, ANCHOR: Web server for predicting protein binding regions in disordered proteins. *Bioinformatics* **25**, 2745–2746 (2009).
54. R. S. Gokhale, C. Khosla, Role of linkers in communication between protein modules. *Curr. Opin. Chem. Biol.* **4**, 22–27 (2000).
55. J. R. Walker, K. A. Severson, M. J. Hermandson, A. Blinkova, K. M. Carr, J. M. Kaguni, *Escherichia coli* DnaA protein: specific biochemical defects of mutant DnaAs reduce initiation frequency to suppress a temperature-sensitive dnaX mutation. *Biochimie* **88**, 1–10 (2006).
56. S. Ozaki, Y. Noguchi, M. Nishimura, T. Katayama, Stable nucleotide binding to DnaA requires a specific glutamic acid residue within the AAA^+ box II motif. *J. Struct. Biol.* **179**, 242–250 (2012).
57. S. Nozaki, T. Ogawa, Determination of the minimum domain II size of *Escherichia coli* DnaA protein essential for cell viability. *Microbiology* **154**, 3379–3384 (2008).
58. S. Kikuchi, I. Shibuya, K. Matsumoto, Viability of an *Escherichia coli* pgsA null mutant lacking detectable phosphatidylglycerol and cardiolipin. *J. Bacteriol.* **182**, 371–376 (2000).
59. D. Camsund, M. J. Lawson, J. Larsson, D. Jones, S. Zikrin, D. Fange, J. Elf, Time-resolved imaging-based CRISPRi screening. *Nat. Methods* **17**, 86–92 (2020).
60. M. W. Parker, M. Bell, M. Mir, J. A. Kao, X. Darzacq, M. R. Botchan, J. M. Berger, A new class of disordered elements controls DNA replication through initiator self-assembly. *eLife* **8**, e48562 (2019).

Acknowledgments

Funding: The Office of the Senior Associate Dean of Faculty and Academic Affairs and the Office of the Dean for Research, Georgetown University Medical Center, provided funding for this study. Partial support was also provided by the Intramural Research Program of CCR, NCI, NIH. **Author contributions:** R.S. conceived the project. Y.H. and R.S., assisted by M.A. and F.S., performed the research. P.K. performed molecular modeling studies. R.S. performed and analyzed the flow cytometry experiments in collaboration with K.M.W. and D.K.C. R.S. wrote the manuscript with input from E.C. and D.K.C. All authors reviewed the results and approved the final version of the manuscript. **Competing interests**: The authors declare that they have no competing interests. **Data and materials availability:** All data needed to evaluate the conclusions in the paper are present in the paper and/or the Supplementary Materials.

Submitted 22 April 2022
Accepted 18 August 2022
Published 5 October 2022
10.1126/sciadv.abq6657